

Design, Synthesis, and Evaluation of Psorospermin/Quinobenzoxazine Hybrids as Structurally Novel Antitumor Agents

Mu-Yong Kim,^{†,‡} Younghwa Na,^{†,‡} Hariprasad Vankayalapati,[†] Mary Gleason-Guzman,[†] and Laurence H. Hurley^{*,†,‡,§}

College of Pharmacy, The University of Arizona, 1703 E. Mabel, Tucson, Arizona 85721, Arizona Cancer Center, 1515 N. Campbell Avenue, Tucson, Arizona 85724, and Department of Chemistry, The University of Arizona, Tucson, Arizona 85721

Received February 26, 2003

Topoisomerase II, an enzyme that catalyzes changes in the topology of DNA, plays several key roles in DNA metabolism and chromosome structure, and it is the primary cytotoxic target for a number of clinically important DNA intercalating agents such as doxorubicin. It seems likely that if these intercalating topoisomerase II poisons are structurally modified to also be DNA alkylating agents, they will have increased dwell time on the topoisomerase II–DNA complex and increased potency and selectivity for cancer cells. On the basis of insights into the mechanisms of action of psorospermin and the quinobenzoxazine A-62176 and molecular modeling studies of these compounds with duplex DNA, we have designed and synthesized a series of novel hybrid DNA-interactive compounds that alkylate DNA most efficiently at sequences directed by topoisomerase II. The epoxydihydrofuran ring of psorospermin was used as a DNA alkylating moiety, and this was fused to the pyridobenzophenoxazine ring of A-62176. The chlorohydrin ring opened form of the epoxide was also prepared and tested. These hybrid compounds showed enhanced DNA alkylating activity in the presence of topoisomerase II, exhibited significant activity against all the cancer cells tested at submicromolar concentrations, and were more potent than both parent compounds. However, the biochemical assays indicated that they lost some of the topoisomerase II and Mg²⁺ dependency for reaction with DNA that is associated with psorospermin and A-62176, respectively.

Introduction

Psorospermin (see Figure 1A for structure) is a novel antitumor antibiotic isolated from the roots and stem-bark of the tropical African plant *Psorospermum febrifugum*.^{1,2} Superficially, psorospermin appears to be mechanistically related to another class of antitumor antibiotics, the pluramycins (see Figure 1B for structure of pluramycin A).^{3,4} Like the pluramycins, psorospermin intercalates into the DNA helix, and the epoxide ring undergoes electrophilic attack by N₇ of guanine (located on the 3'-side of the drug molecule), creating a lesion that is cationic in nature and therefore may depurinate inside cells (Figure 1C).⁵ However, to achieve maximum stabilization within the DNA helix, psorospermin must intercalate parallel to the helix axis, while the pluramycins must intercalate perpendicularly.⁵ In contrast to the pluramycins, psorospermin has no carbohydrate substituents and thus shows poor sequence specificity and low reactivity toward duplex DNA. However, psorospermin has at least in vitro cytotoxic potency equal to that of the pluramycins in the NCI 60-panel screen. This apparent paradox was rationalized by the observation that the alkylation reactivity of psorospermin with specific DNA sequences is significantly increased in the presence of topoisomerase II.⁶ On the basis of this observation, a model was proposed

in which topoisomerase II induces structural distortion at its binding sites, allowing the reactive epoxide ring of psorospermin to become more proximal to N₇ of guanine and/or to stabilize the noncovalently bound psorospermin. This leads to the selective DNA alkylation by psorospermin of N₇ of guanine within the topoisomerase II–DNA gate sites.⁶

Topoisomerase II is an enzyme that catalyzes changes in the topology of DNA via a mechanism that involves the transient double-strand breaking and rejoining of phosphodiester bonds.^{7,8} This enzyme plays several key roles in DNA metabolism and chromosome structure,⁹ and it is the primary molecular target for a number of potent anticancer drugs. Most of the clinically useful drugs that interact with the binary topoisomerase II–DNA complex are known as topoisomerase II poisons and interfere with the breaking–rejoining reaction of the enzyme by trapping the reaction intermediate, the covalent topoisomerase II–DNA complex. This complex is normally short-lived under physiological conditions.^{10–16} The efficacy of a drug is highly dependent on its dwell time within the ternary topoisomerase II–DNA–drug complex because once the drug dissociates from the complex, the reaction proceeds unhindered to its fruition. Thus, compounds that irreversibly trap the topoisomerase II–DNA complex might have a clinical advantage associated with a more potent cytotoxic effect toward cancer cells.¹⁷

A-62176 (see Figure 1A for structure) is a fluoroquinolone analogue that shows good activity against a number of cancer cell lines.^{18–20} A self-assembly model

* To whom correspondence should be addressed. Phone: 520 626-5622. Fax: 520 626-5623. E-mail: hurley@pharmacy.arizona.edu.

[†] College of Pharmacy, The University of Arizona.

[‡] These authors contributed equally to this manuscript.

[§] Arizona Cancer Center.

[§] Department of Chemistry, The University of Arizona.

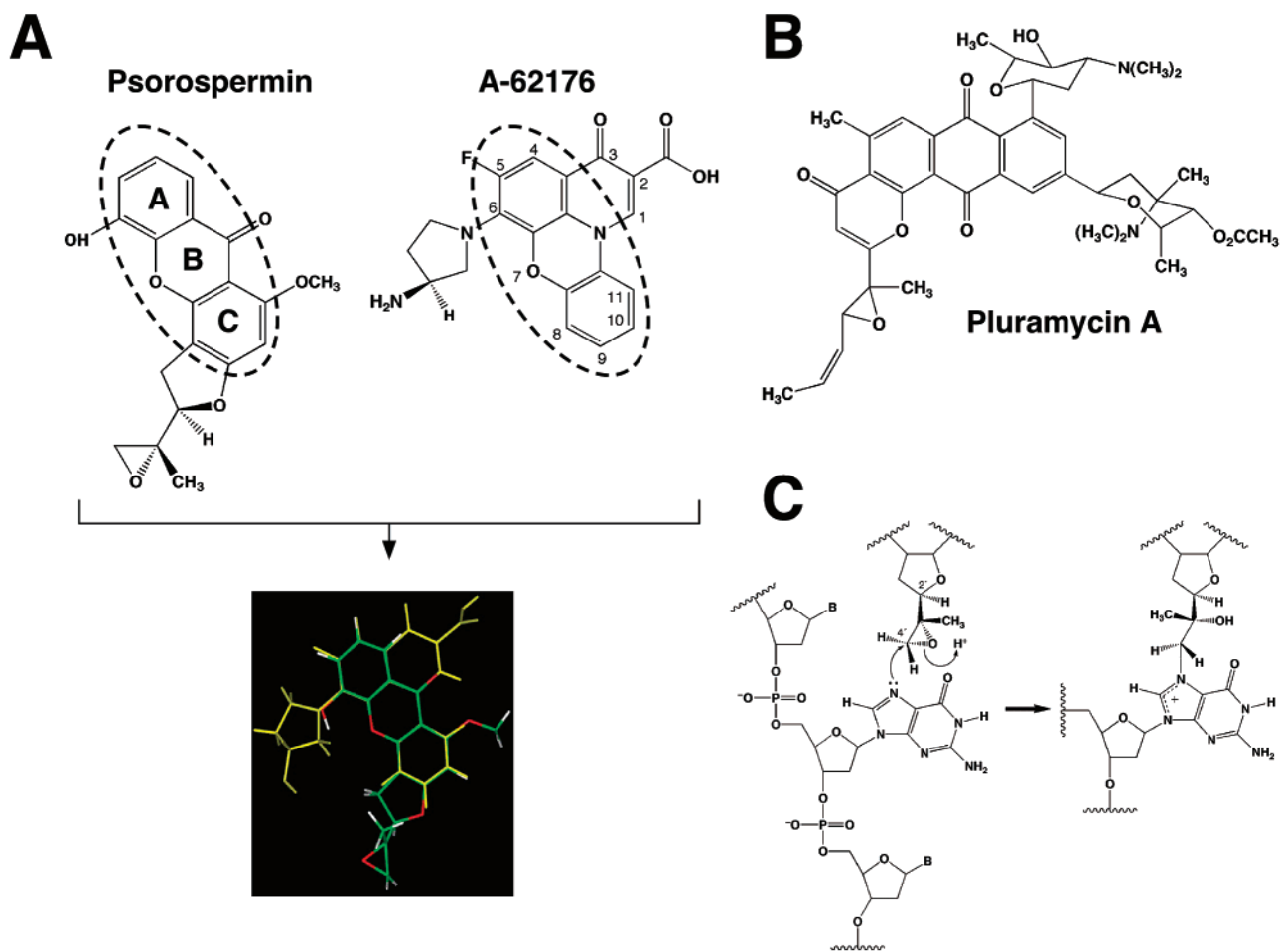


Figure 1. (A) Structures of psorospermin and A-62176 and view of the field fit alignment model of psorospermin (color by atom) and A-62176 (yellow). (B) Structure of pluramycin A. (C) Summary of the proposed mechanism of covalent modification of DNA by psorospermin to form the psorospermin-(N₇ guanine)-DNA adduct. The drug molecule intercalates the DNA molecule to position the reactive epoxide into the major groove to perform site-directed electrophilic addition on N₇ of guanine.

has been proposed for A-62176 on the basis of the results from previous biophysical and biochemical studies.^{21,22} In this model, a 2:2 drug-Mg²⁺ dimer binds to DNA, with one drug molecule intercalated into DNA base pairs and the second drug molecule externally bound through two chelated Mg²⁺ ions. Two magnesium cations link the two drug molecules in a head-to-tail fashion such that the bidentate ligand of the β -keto acid moiety and the primary amino group of the aminopyrrolidine side chain are the head and tail, respectively. Each magnesium cation also binds with one phosphate oxygen of the DNA backbone and two water molecules to form an octahedral complex. Previously, it was demonstrated that A-62176 competes with psorospermin within the topoisomerase II-DNA complex.²³ The steric and electronic similarities between psorospermin and A-62176 (see dashed ovals in Figure 1A) suggested to us that they might overlap within the intercalation site in the duplex DNA and interact similarly with the topoisomerase II-DNA complex.

On the basis of the similar chemical structures of psorospermin and A-62176 and molecular modeling studies of these compounds bound to duplex DNA, we have designed and synthesized a series of new DNA-interactive agents that are more efficient at making irreversible DNA adducts at the topoisomerase II binding sites than the source molecules. The biological

activity of the new compounds was determined with respect to *in vitro* cytotoxicity against a variety of cancer cell lines.

Results

A-62176 and Psorospermin Are Structurally Similar. A-62176 competes with psorospermin for binding to the *Drosophila* topoisomerase II-DNA complex,^{6,23} suggesting that psorospermin and A-62176 may have similar binding modes that involve direct interactions at the same DNA intercalation sites. To determine the structural similarities between psorospermin and A-62176, the three-dimensional structures of these two compounds were compared using field fit atom-atom superimposition (Figure 1A). The superimposition of these two molecules revealed that there is substantial structural overlap; in particular, their aromatic portions and H-bond acceptors, such as the 6-oxo atom of A-62176 and the xanthone oxygen of psorospermin, are in good alignment. The field fit alignment yields a similarity function of 0.57 Å rmsd, reflecting a minimized structural variation between the two molecules. This result suggests that psorospermin and A-62176 present a common pharmacophore to their intracellular target, presumably the topoisomerase II-DNA complex.

Human Topoisomerase II Enhances the DNA Alkylating Activity of Psorospermin under Physi-

ological Conditions, and A-62176 Competes with Psorospermin for this Reaction. Previously it was found that the DNA alkylating activity of psorospermin is significantly increased at specific sites of DNA in the presence of *Drosophila* topoisomerase II.⁶ On the basis of these results, it was envisaged that topoisomerase II could change the conformation of duplex DNA and thereby create a site that is favorable for alkylation by psorospermin. However, these studies were carried out with *Drosophila* topoisomerase II under acidic conditions (pH 6.0). Thus, in the current study, experiments were designed to verify the mechanism of DNA alkylation by psorospermin in the presence of human topoisomerase II at pH 7.6, conditions that are more analogous to those in the intracellular environment. A 60-base-pair duplex DNA, which contains two sets of topoisomerase II cleavage sites (see Figure 2D), was incubated with increasing concentrations of psorospermin in the presence and absence of human topoisomerase II for 20 min at 30 °C.⁶ Piperidine heat treatment of the samples was then used to generate strand-breakage products, which result from depurination of the N₇-alkylated guanine. In the absence of human topoisomerase II, there was only a weak, nonspecific alkylation of DNA by psorospermin (Figure 2A, lanes 5 and 6). However, in the presence of human topoisomerase II, significantly greater DNA alkylation was observed at one specific guanine site (Figure 2A, lanes 8 and 9), which is located at one of the topoisomerase II mediated cleavage sites (+4' position of site B in Figure 2D). In a previous study, no significantly enhanced cleavage in the presence of topoisomerase II was found on the other strand.⁶ The results reported here are consistent with the results from the earlier study using *Drosophila* topoisomerase II under acidic conditions.⁶

In the previous section, we suggested that psorospermin and A-62176 might present a common pharmacophore to the topoisomerase II–DNA complex. To test this hypothesis, a competition study between psorospermin and A-62176 was carried out in the presence of human topoisomerase II. As the concentration of A-62176 was increased, the amount of psorospermin-mediated DNA alkylation decreased significantly (Figure 2B, lanes 2–5), demonstrating that A-62176 most likely competes with psorospermin for binding within the same topoisomerase II–DNA target site. Less likely is the possibility that A-62176 binds to a proximal site to inhibit the topoisomerase II induced psorospermin alkylation.

To determine whether it was the binding of topoisomerase II that enhanced the DNA alkylating activity of psorospermin at the specific DNA site, a topoisomerase II mediated DNA cleavage assay was carried out using SDS and proteinase K treatment.²³ During the DNA breaking and rejoining process, the topoisomerase II enzyme is known to form a covalent bond with the cleaved DNA, resulting in the formation of a transient topoisomerase II–DNA complex.^{7,8} If psorospermin does indeed bind to the topoisomerase II–DNA complex, it would then alkylate the DNA at its binding site and therefore interfere with the DNA rejoining reaction of topoisomerase II. This would result in increased amounts of DNA cleavage product at this enzyme's binding site, which can then be trapped and quantified using SDS

and proteinase K treatment. We found that the intensity of topoisomerase II mediated DNA cleavage increased in a concentration-dependent manner for psorospermin (lanes 2–7 in Figure 2C, black triangle; +1' position in Figure 2D). This cleavage at a cytosine is located in proximity to the guanine (+4' position in Figure 2D) that was found to be preferentially alkylated by psorospermin in the presence of topoisomerase II. Psorospermin acts as a catalytic inhibitor at site A (lanes 2–7 in Figure 2C, white triangle). Therefore, taken together, these results are consistent with the enhanced DNA alkylating activity of psorospermin being due to topoisomerase II binding at a specific DNA site, which induces a structural distortion around its binding site.

Structural Docking of Psorospermin and A-62176 with Duplex DNA. In the previous section, we demonstrated that human topoisomerase II binds to specific DNA sites and induces the DNA alkylating activity of psorospermin under physiological conditions. A detailed analysis of the interaction of psorospermin with the topoisomerase II–DNA complex requires a crystal structure of the ternary topoisomerase II–DNA–drug complex, but this is unavailable. However, the high-resolution crystal structure (1.50 Å) of doxorubicin bound to d[CGTAC5G6/C7G8TACG] is available, and this was used as a starting structure for building the initial model of the psorospermin–DNA complex.²⁴ Psorospermin was manually inserted into the doxorubicin intercalation site at C5G6 using a field fit alignment affinity docking experiment. The structure of the complex was then submitted to a series of simulated annealing (SA) docking experiments, as detailed in the Experimental Section. The most stable dynamic trajectory reveals that the xanthone ring of psorospermin intercalates into DNA base pairs in a parallel orientation in which the A-ring of psorospermin exhibits a stable stacking interaction with G8, and its –OH group has a close contact with the carbonyl oxygen of G8 (Figure 3A). The ether oxygen of the xanthone ring and the carbonyl oxygen of the B-ring show charge–charge interactions with the 2-amino group of G8, and the –OCH₃ group in the C-ring is involved in several van der Waals contacts with G6 (distance of 3.4 Å). In this model, the stacking interactions of the benzofuran oxygen atom and the 3'R methyl group with the G8 base are probably unfavorable because of a local 25° twist at the 2-substituted oxiranyl moiety. The proximity of the –CH₂ of epoxide ring to N₇ of G6 was calculated because N₇ of guanine would attack this methylene group to form a DNA adduct. The distance between the two groups was found to be 3.95 Å. To confirm the stability of the psorospermin–DNA complex, we performed a molecular dynamics (MD) simulation at 100 ps in a hydrated system. It was found that the position and orientation of psorospermin were similar to those observed in the previous SA docking simulations. The only difference identified was that the binding energy is increased from –46.71 to –53.96 kcal/mol. This suggests that the SA docking simulations could be used to predict the stable psorospermin–DNA complex structure.

The binding mode of A-62176 was analyzed using the psorospermin–DNA complex structure. A-62176 shows

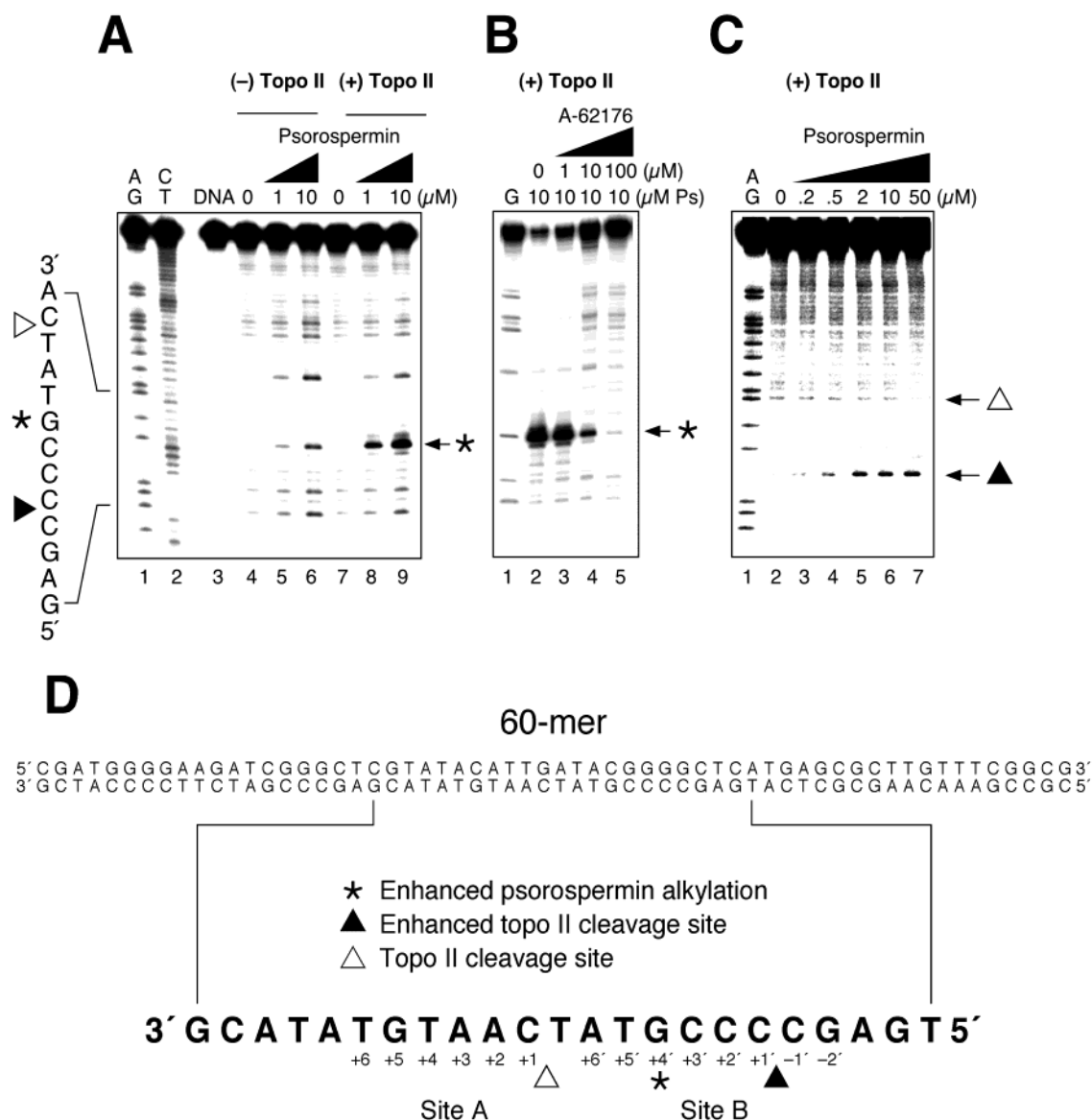


Figure 2. Effect of human topoisomerase II on the extent of alkylation of DNA by psorospermin. (A) Autoradiograms of denaturing polyacrylamide gels showing the DNA strand-breakage patterns produced by psorospermin. Lanes 1 and 2 contain the Maxam–Gilbert sequencing reactions of AG and TC. Lane 3 is control DNA without heat treatment. Lanes 4–6 contain 0, 1, and 10 μM of psorospermin in the absence of topoisomerase II. Lanes 7–9 contain 0, 1, and 10 μM of psorospermin in the presence of topoisomerase II. The sequence to the left shows the psorospermin alkylation site (asterisk) and topoisomerase II cleavage sites A (white triangle) and B (black triangle). (B) Competition assay between psorospermin and A-62176. The topoisomerase II–DNA complex was formed, as described in the Experimental Section, in the presence of various concentrations of A-62176. Psorospermin (10 μM) was added to the reaction mixture, and the reaction continued for another 20 min, followed by piperidine treatment. Lane 1 contains the Maxam–Gilbert sequencing reaction of G. Lanes 2–5 contain 0, 1, 10, and 100 μM A-62176 in the presence of 10 μM psorospermin (Ps) and topoisomerase II. The psorospermin alkylation site is indicated by an asterisk. (C) Effect of psorospermin on DNA cleavage activity of human topoisomerase II. Autoradiogram of a denaturing polyacrylamide gel showing the topoisomerase II mediated DNA cleavage pattern in the presence of psorospermin. Lane 1 contains the Maxam–Gilbert sequencing reaction of AG. Lanes 2–7 contain 0, 0.2, 0.5, 2, 10, and 50 μM of psorospermin in the presence of topoisomerase II. The topoisomerase II cleavage sites are shown to the right of the gel (site A = white triangle, site B = black triangle). (D) Oligomers used for DNA alkylation and topoisomerase II mediated DNA cleavage assays. To precisely define the location of the bases at the topoisomerase II cleavage sites, positive and negative numbers (+6 ... +1 for site A and +6' ... -2' for site B) are used on the bottom strand to indicate the bases at which phosphodiester bonds are cleaved on the 3' and 5' sides by topoisomerase II. In all the experiments, the bottom strand was 5'-end-labeled.

good stacking interactions at the same DNA binding site of psorospermin (Figure 3B). The presence of an additional fused ring at the quinolone nitrogen position and the 3-aminopyrrolidine ring at position 6 (Figure 1) provides additional stacking interactions with the C5G6 step, with the quinolone nitrogen substituent located in the major groove and the C6 substituent located in the minor groove between C5 and G8. The

2-carboxylic acid moiety of A-62176 further stabilizes the complex through Mg^{2+} ion coordination. In the case of A-62176, the distances between the Mg^{2+} ion and the 3-carbonyl and 2-carboxylic acid are 4.74 and 7.26 Å, respectively.

Design of New Hybrid Compounds Based on the Molecular Modeling Studies. On the basis of results from the SA docking and MD simulations of psorosper-

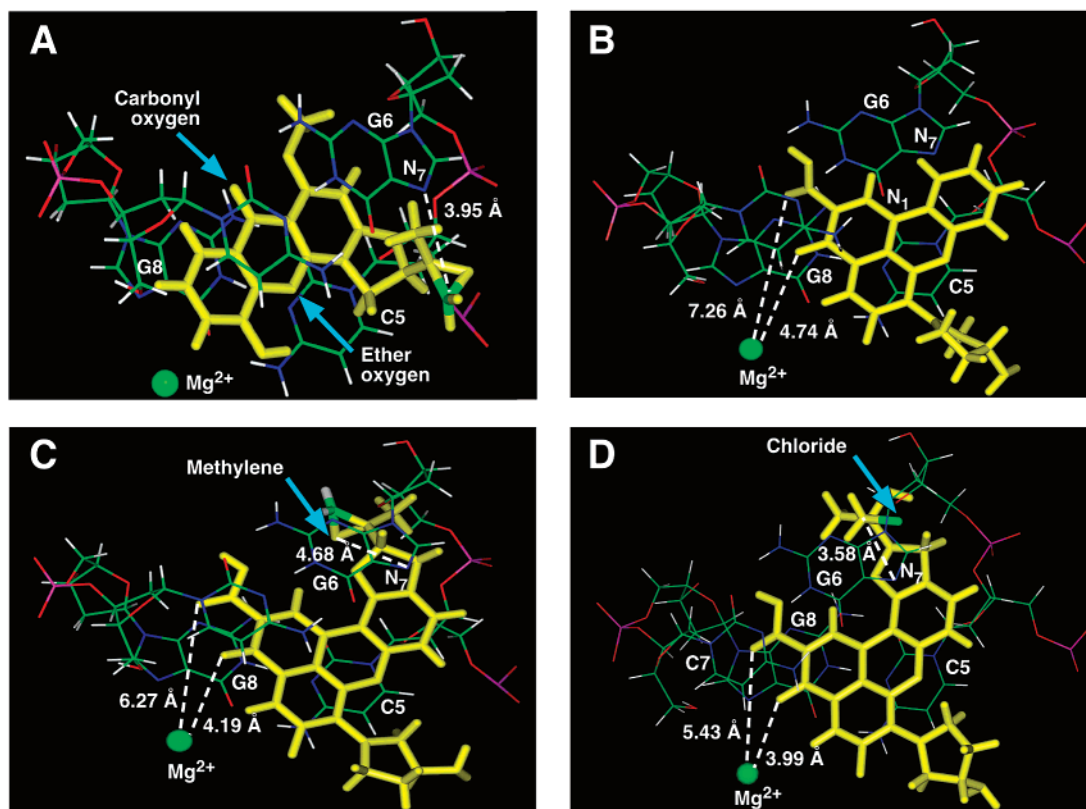
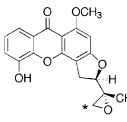
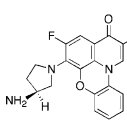
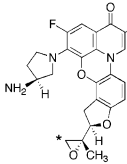
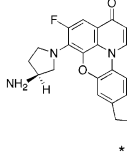
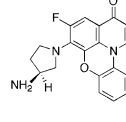
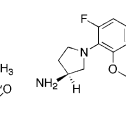


Figure 3. Molecular models of the view from the C5G6 base pair (color-by-atom type) depicting the mode of binding and stacking for psorospermin (A), A-62176 (B), hybrid epoxide-3 (C), and hybrid chlorohydrin-4 (D). The distances between N₇ of G6 (blue) and the -CH₂ atoms (green) were found to be 3.95 Å for psorospermin, 4.68 Å for hybrid epoxide-3, and 3.58 Å for hybrid chlorohydrin-4 (white dashed lines). The Mg²⁺ ion coordination distances composed of sp² and carboxyl oxygens are also shown.

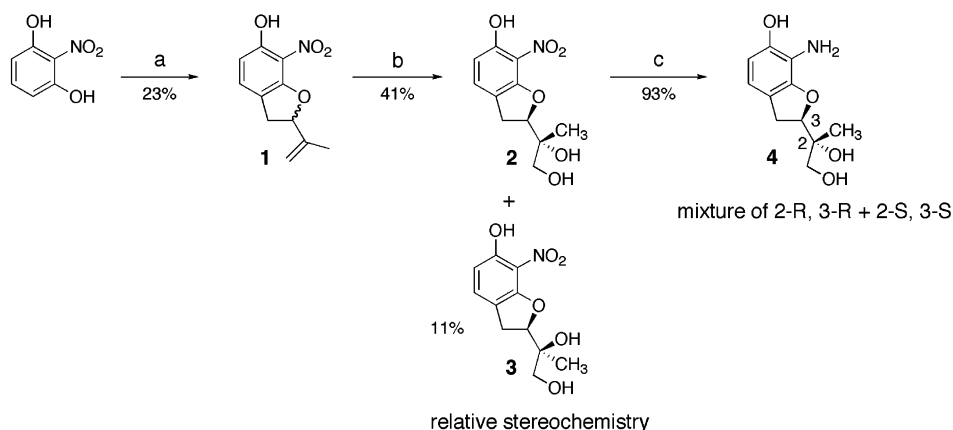
Table 1. Computed Binding Energies and Distances between N₇ of Guanine and the Alkylated Carbon for the d[(C5G6)/(C7G8)] Complexes of Psorospermin, A-62176, and the Hybrid Compounds

						
	Psorospermin	A-62176	Hybrid epoxide-1	Hybrid epoxide-2	Hybrid epoxide-3	Hybrid chlorohydrin-4
Distance (Å) ^a	3.95	—	6.96	6.51	4.68	3.58
Binding energy ^b	-53.96	-43.78	-46.19	-29.83	-61.23	-73.86

^a -CH₂* and N₇ of guanine. ^b In kcal/mol.

min described in the previous section, we propose that upon binding to the duplex DNA, topoisomerase II induces a structural distortion at its binding site. This structural distortion in duplex DNA allows the planar portion of psorospermin to form more favorable π - π stacking interactions with the DNA base pairs. As a result, the distance between the -CH₂ of the epoxide ring of psorospermin and N₇ of guanine is reduced to less than 3.95 Å, which serves to greatly increase DNA alkylation of N₇ of guanine by psorospermin within the topoisomerase II-DNA gate sites. On the basis of this model, we have designed a series of psorospermin/quinobenzoxazine hybrid compounds with the aim of

combining the selectivity imparted by the topoisomerase II induced alkylation of DNA and the Mg²⁺ dependency of A-62176. The epoxydihydrofuran of psorospermin was appended as a DNA alkylating moiety to the pyrido-benzophenoxazine ring of A-62176 at the three possible positions (Table 1), and the binding of these compounds with DNA was investigated using SA docking and MD simulations. In the case of hybrid epoxide-1 (Table 1), the epoxydihydrofuran moiety had a strong steric clash with the sugar phosphate group of C5. The distance between -CH₂ of the epoxide of hybrid epoxide-1 and N₇ of guanine was 6.96 Å, which is an increase of 2.14 Å in comparison with the equivalent distance for pso-

Scheme 1^a

^a (a) 2-Methyl-*trans*-1,4-dibromo-2-butene, *n*-BuLi toluene room temp -110 °C; (b) NMO catalyst, OsO₄, CHCl₃/acetone/H₂O, room temp; (c) MeOH Pd(C), H₂, room temp.

rospermin (Table 1). Hybrid epoxide-2 also showed an increase in the distance between the two groups (6.51 Å) due to the position of the epoxide ring. In contrast to hybrid epoxide-1 and hybrid epoxide-2, hybrid epoxide-3 exhibited a reduced distance between $-CH_2$ of the epoxide ring and N₇ of guanine (4.68 Å), but this is still more than it is in psorospermin. The tricyclic phenoxazine ring of hybrid epoxide-3 is intercalated between C5 and G6, and its 6-fluorophenyl ring has additional stacking interactions with G8 (Figure 3C). The central 6-oxo ring is positioned within 3.5–4.2 Å of the C5 and G6 bases, and the oxygen atom in the benzofuran ring shows three van der Waals contacts with N₃, N₇, and N₉ of G6. The distances between the Mg²⁺ ion and 3-carbonyl and 2-carboxylic acid of hybrid epoxide-3 were 4.19 and 6.27 Å, respectively, indicating a strong coordination compared to A-62176. Such metal coordination suggested an additional feature for stabilization of the complex in the case of hybrid epoxide-3. Unlike psorospermin, the $-CH_2$ group of epoxide in hybrid epoxide-3 is not involved in steric interactions with G6. Hence, hybrid epoxide-3 shows a higher binding energy (Table 1) with DNA base pairs (-61.23 kcal/mol) compared to psorospermin, which would extend the dwell time of the compound in the molecular target and thereby increase the chance of alkylation.

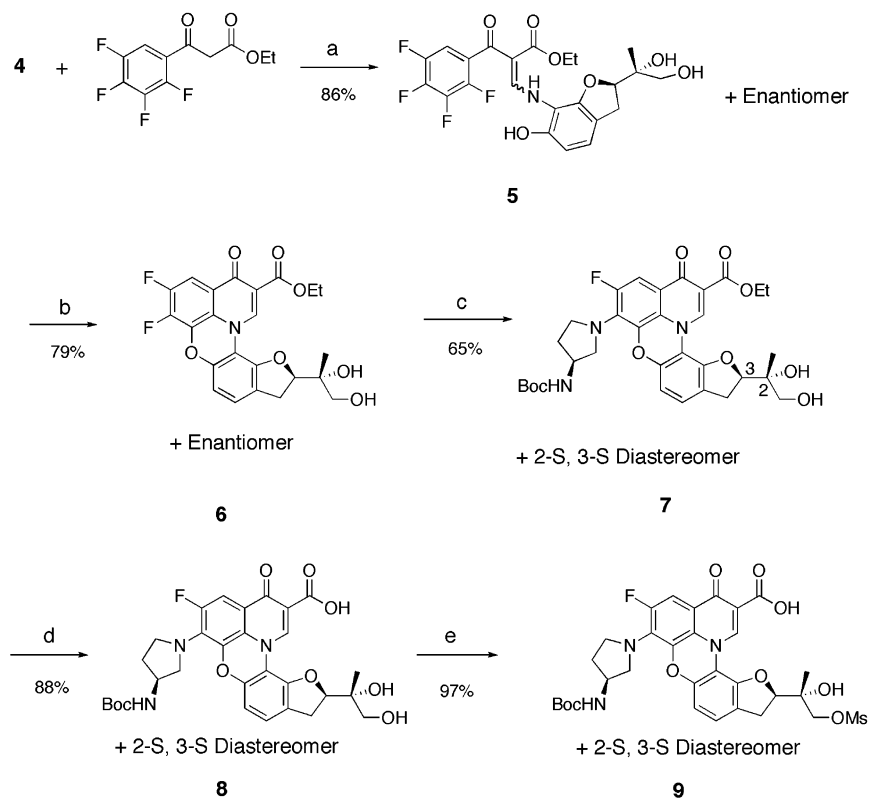
The reactive epoxide attached at the furan ring of hybrid epoxide-3 was then substituted with a chlorohydrin group (Table 1), which would be anticipated to display different accessibility and nucleophilicity toward N₇ of guanine. The chlorohydrin moiety and phenoxazine ring of hybrid chlorohydrin-4 show increased stacking interactions between the C7 and G8 bases, and these stacking interactions slightly change the position of the benzofuran ring that is planar to C5 (Figure 3D). Thus, the chloride atom of chlorohydrin is close to G6 and has a decreased distance between $-CH_2$ of chlorohydrin and N₇ of G6 (3.58 Å) in comparison to both psorospermin and hybrid epoxide-3.

Synthesis of the Designed Hybrid Compounds.

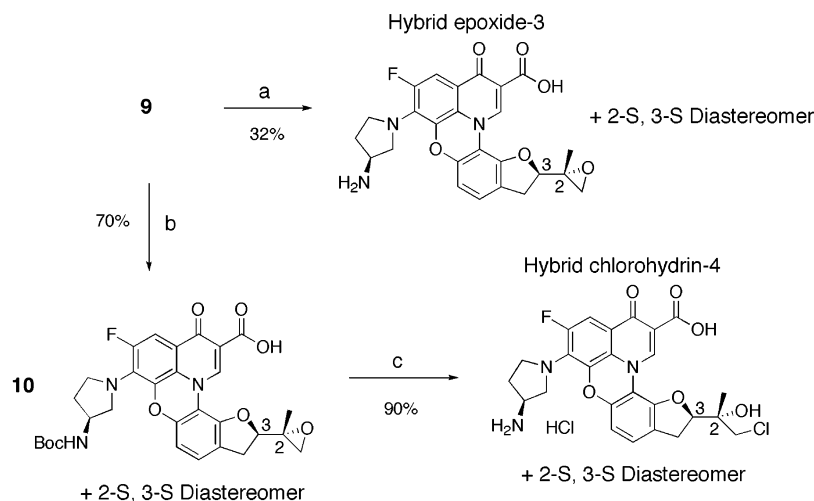
On the basis of the above considerations, hybrid epoxide-3 and hybrid chlorohydrin-4 were synthesized (Schemes 1–3) on the basis of published methods for the construction of quinobenzoxazines and psorospermin methyl ether,^{25–27} with modifications. We chose compound 4 as a convenient intermediate to form the

psorospermin-like portion of the target compounds, prepared in three steps using known methods (Scheme 1).²⁵ First, treatment of 2-nitroresorcinol with 2-methyl-*trans*-1,4-dibromo-2-butene with *n*-BuLi as a base afforded compound 1, producing the dihydrobenzofuran ring system in one step but in low yield (23%). Dihydroxylation of compound 1 with NMO and OsO₄ generated two enantiomeric mixtures of diastereomers 2 and 3, with some selectivity for the desired isomers 3. The diastereomers were separated using PTLC (10% MeOH–CHCl₃), and the relative stereochemistry was assigned on the basis of information from the literature.²⁶ Compound 4 was obtained after catalytic hydrogenation of the separated isomers 3. Literature methods were again employed for the preparation of the final structures of hybrid epoxide-3 and hybrid chlorohydrin-4 (Scheme 2).^{26,27} Compound 4 was coupled with ethyl 2,3,4,5-tetrafluorobenzoylacetate in triethyl orthoformate and acetic anhydride to give compound 5, and consecutive double cyclization under basic (NaHCO₃) conditions furnished the entacyclic compound 6 as an enantiomeric mixture. Regioselective nucleophilic substitution of the fluorine in the C-1 position in compound 6 with optically pure 3(*S*)-(tert-butoxycarbonylamino)pyrrolidine was achieved under reflux in pyridine to provide compound 7 as a 1:1 diastereomeric mixture in moderate yield. Further elaboration by hydrolysis followed by mesylation of the primary alcohol generated key intermediate 9. Hybrid epoxide-3 was obtained, again as a diastereomeric mixture, after *t*-Boc deprotection followed by epoxide formation with *t*-BuOK. In the ¹H NMR of hybrid epoxide-3, we observed two doublet signals at 2.77 (1H, *J* = 4.1 Hz) and 2.88 (1H, *J* = 4.1 Hz) ppm, characteristic of the two methylene protons in the epoxide ring and consistent with the values of those in the psorospermin epoxide ring.²⁶ Hybrid chlorohydrin-4 was generated by epoxide formation (K₂CO₃/acetone) from compound 9, followed by concomitant *t*-Boc deprotection and hydrolysis under acid (1 N HCl/EtOAc) conditions (Scheme 3).

Hybrid Epoxide-3 Shows Enhanced DNA Alkylation but Less Selective Topoisomerase II Induced Alkylation. The DNA alkylating activity of hybrid epoxide-3 was compared with that of psorospermin in the presence and absence of topoisomerase II. Piperidine heat treatment was used to generate the

Scheme 2^a

^a (a) $\text{CH}(\text{OEt})_3$, Ac_2O , 130°C 4 h then 4, pyr, CHCl_3 , room temp, 17 h; (b) NaHCO_3 , DMF, 110°C , 2 h; (c) 3(*S*)-(tert-butoxycarbonylamino)pyrrolidine, pyr, 110°C ; (d) EtOH, 1 N KOH, 80°C ; (e) Pyr, MsCl, 0°C 30 min.

Scheme 3^a

^a (a) HCl, EtOAc, room temp, then *t*-BuOK in BuOH; (b) 18-C-6, K_2CO_3 , acetone, room temp; (c) aqueous HCl, EtOAc, room temp.

strand-breakage products resulting from depurination of the N_7 -alkylating guanine.⁶ In the absence of topoisomerase II, there was only weak alkylation of DNA by psorospermin (lane 4 in Figure 4A and Figure 4B). However, significantly greater DNA alkylation was observed at most guanines by hybrid epoxide-3 (lane 6 in Figure 4A; see all sites except E and H in Figure 4C). In the presence of topoisomerase II, psorospermin shows just one site of preferentially induced DNA alkylation at the guanine (lane 5 in Figure 4A; see site F in Figure 4B). In contrast, the presence of topoisomerase II served to increase significantly the DNA alkylating activity of hybrid epoxide-3 at all the guanines (lane 7 in Figure

4A; Figure 4C). The observation that hybrid epoxide-3 strongly alkylates DNA, even in the absence of topoisomerase II, may simply be due to the greater intrinsic binding interactions of this compound. In contrast to psorospermin, hybrid epoxide-3 shows fairly indiscriminant topoisomerase II induced DNA alkylating activity at guanines, indicating that hybrid epoxide-3 has less topoisomerase II induced alkylation specificity than psorospermin.

Hybrid Chlorohydrin-4 Shows Enhanced DNA Alkylation at Higher pH Conditions. The DNA alkylating activity of hybrid chlorohydrin-4 was also measured. Hybrid chlorohydrin-4 did not induce DNA

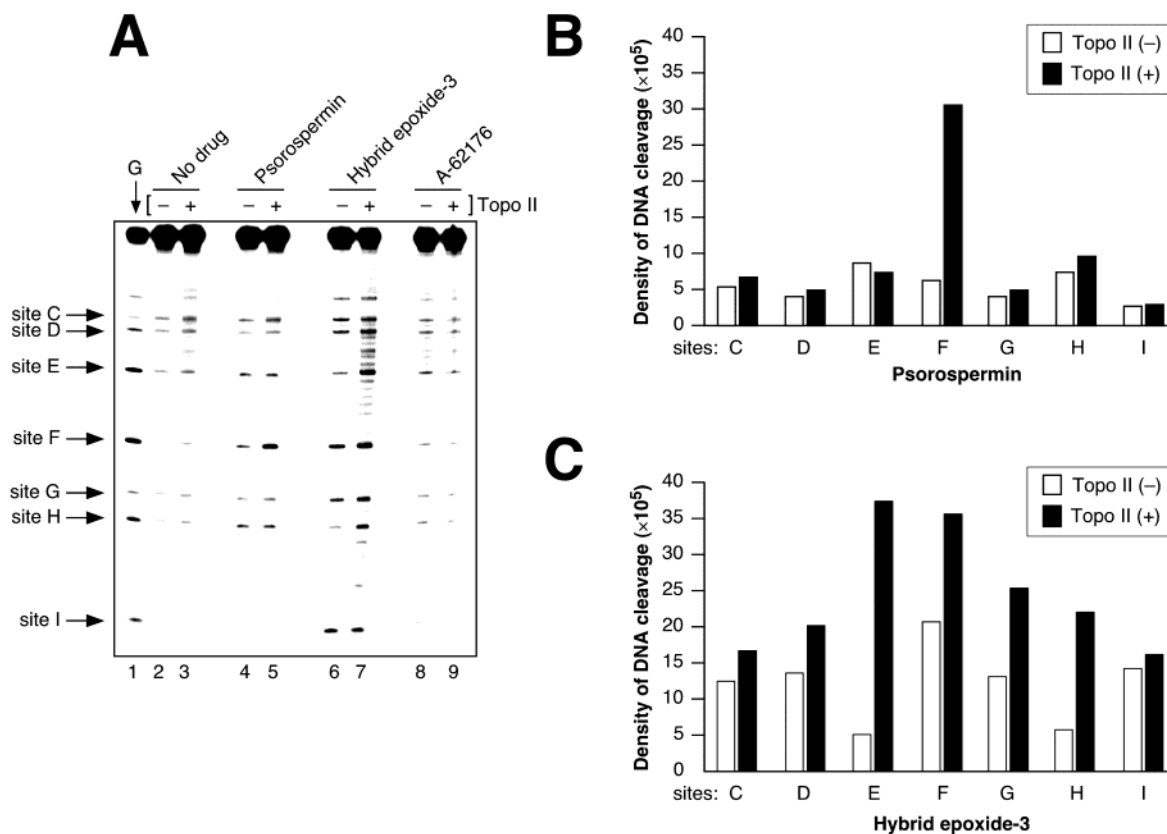


Figure 4. DNA alkylating activities of psorospermin, hybrid epoxide-3, and A-62176. (A) Autoradiograms of denaturing polyacrylamide gels showing the DNA alkylation patterns produced by psorospermin, hybrid epoxide-3, and A-62176. Lane 1 contains the Maxam–Gilbert sequencing reaction of G. Lanes 2 and 3 contain no drug. Lanes 4 and 5, 6 and 7, and 8 and 9 contain 10 μ M of psorospermin, hybrid epoxide-3, and A-62176, respectively. Lanes 3, 5, 7, and 9 contain topoisomerase II. To the left of the gel are the sites (C–I) of covalent adduct formation. (B and C) Graphical representations of the quantification of the gels shown in (A). Sites C–I refer to those shown in (A).

alkylation relative to that of hybrid epoxide-3 (Figure 5A; compare lanes 4 and 5 with lanes 6 and 7). To further characterize the DNA alkylating activity of hybrid chlorohydrin-4, the same experiment was carried out at higher pH conditions, which are more favorable for nucleophilic displacement of the chloride. At pH 9.0, alkylation was observed for hybrid chlorohydrin-4, and the intensity was increased in a pH-dependent manner (Figure 5B).

Hybrid Chlorohydrin-4 Does Not Show Mg²⁺ Dependency for DNA Binding. Previously it was shown that the ability of A-62176 to bind to DNA is dependent upon the presence of Mg²⁺.²¹ To compare the potential dependency of A-62176 and hybrid chlorohydrin-4 on Mg²⁺ for binding to duplex DNA, a spectrophotometric assay was used.²¹ In the absence of DNA, A-62176 showed an absorption peak at 315 nm (Figure 6A). Upon addition of DNA to a solution of A-62176, there was very little change in the intensity of this absorption peak; however, in the presence of Mg²⁺, a significant decrease in this absorption peak was observed (parts B and C of Figure 6), presumably due to intercalation. In contrast, the incremental addition of DNA to the hybrid chlorohydrin-4 solution caused a significant reduction in the absorption peak of the compound in both the absence and presence of Mg²⁺ (Figure 6D–F). These results suggest that hybrid chlorohydrin-4 does not require Mg²⁺ for binding with duplex DNA, which may be because of the higher intrinsic binding energy of hybrid chlorohydrin-4 to

DNA (–73.86 kcal/mol) compared to that of A-62176 (–43.78 kcal/mol).

Hybrid Compounds Show More Potent Cytotoxicity Than Psorospermin and A-62176 against Various Cancer Cell Lines. The antiproliferative activity of the hybrid compounds was compared to that of psorospermin and A-62176 against 10 different cancer cell lines (Table 2). The hybrid compounds showed significantly more potent activity than psorospermin and A-62176. Hybrid chlorohydrin-4 was slightly more active than hybrid epoxide-3. Hybrid epoxide-3 and hybrid chlorohydrin-4 displayed potent activity against all the cancer cells at submicromolar concentrations, particularly against DU145 prostate, H522 NSCLS cancer cells, U937 lymphoma, and Granta lymphoma. Hybrid chlorohydrin-4 was 10- to 20-fold more potent than psorospermin against most cancer cell lines tested.

Discussion

Anticancer agents that alkylate DNA are some of the most effective drugs in the clinic and have significantly increased the survival rate of cancer patients. Unfortunately these drugs are not selective for cancer cells and serve to adversely affect certain critical cellular functions of normal and tumor cells alike.²⁸ In contrast to these nonspecific DNA alkylating agents, anticancer agents that interact with the protein–DNA complexes (for example, topoisomerase II poisons) have greater selectivity for cancer cells over normal cells.¹⁷ DNA-

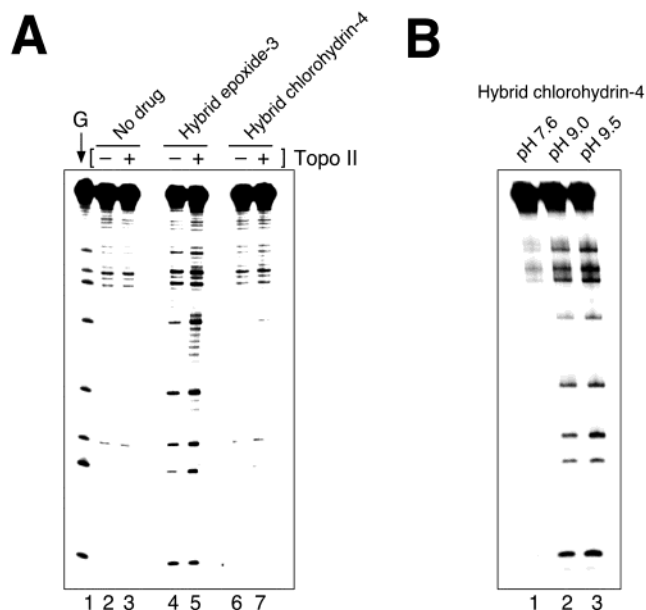


Figure 5. DNA alkylating activities of hybrid epoxide-3 and hybrid chlorohydrin-4. (A) Alkylation of hybrid epoxide-3 and hybrid chlorohydrin-4 at pH 7.6. Lane 1 contains the Maxam-Gilbert sequencing reaction of G. Lanes 2 and 3 are without drug. Lanes 4 and 5 and 6 and 7 contain $10 \mu\text{M}$ of hybrid epoxide-3 and hybrid chlorohydrin-4, respectively. Lanes 3, 5, and 7 contain topoisomerase II. (B) Effect of pH on topoisomerase II mediated DNA alkylation of hybrid chlorohydrin-4. Lanes 1–3 were incubated for 1 h in Tris buffer (pH 7.6), glycine-NaOH buffer (pH 9.0), and glycine-NaOH buffer (pH 9.5), respectively.

interactive drugs that target topoisomerase II–DNA complexes have greater selectivity for cancer cells because elevated levels of topoisomerase II are associated with higher rates of replication of tumor cells.¹⁰

These drugs bind to and stabilize the transient topoisomerase II–DNA complex, which is then stabilized as a ternary topoisomerase II–DNA–drug complex. The dwell time of drugs in this ternary complex is very important for their efficacy as anticancer agents.¹⁷ Thus, the compounds that irreversibly trap the topoisomerase II–DNA complex are likely to have the greatest cytotoxic potency, and perhaps selectivity, for cancer cells.²⁹

The objective of this study was the design, synthesis, and evaluation of new DNA alkylation agents that form irreversible DNA adducts with the topoisomerase II–DNA complex. Psorospermin and A-62176 served as templates for the design of the new agents. SA docking and MD simulations of psorospermin and A-62176 within the complex enabled the identification of structures that possess optimal π – π stacking interactions and alkylating properties. Hence, an initial series of novel hybrid compounds (hybrid epoxide-1, -2, and -3) that have an epoxydihydrofuran ring of psorospermin as a DNA alkylating moiety and the pyridobenzophenoxazine ring of A-62176 as a pharmacophore were designed. Hybrid epoxide-3 was expected to have the best accessibility to N_7 of guanine and the most stable binding interactions among this series of hybrid compounds, and therefore, this compound was synthesized and analyzed for DNA alkylating activity and cytotoxicity. Hybrid epoxide-3 showed potent DNA alkylating activity and enhanced cytotoxicity compared to the two parent compounds. The results from this study are consistent with specific molecular features of psorospermin and hybrid epoxide-3 that are critical for optimal activity. These include the planar nature of both molecules and their reactive epoxide moieties. Psorospermin has insufficient π – π stacking interactions to enable its epoxide ring to alkylate N_7 of guanine. However, hybrid

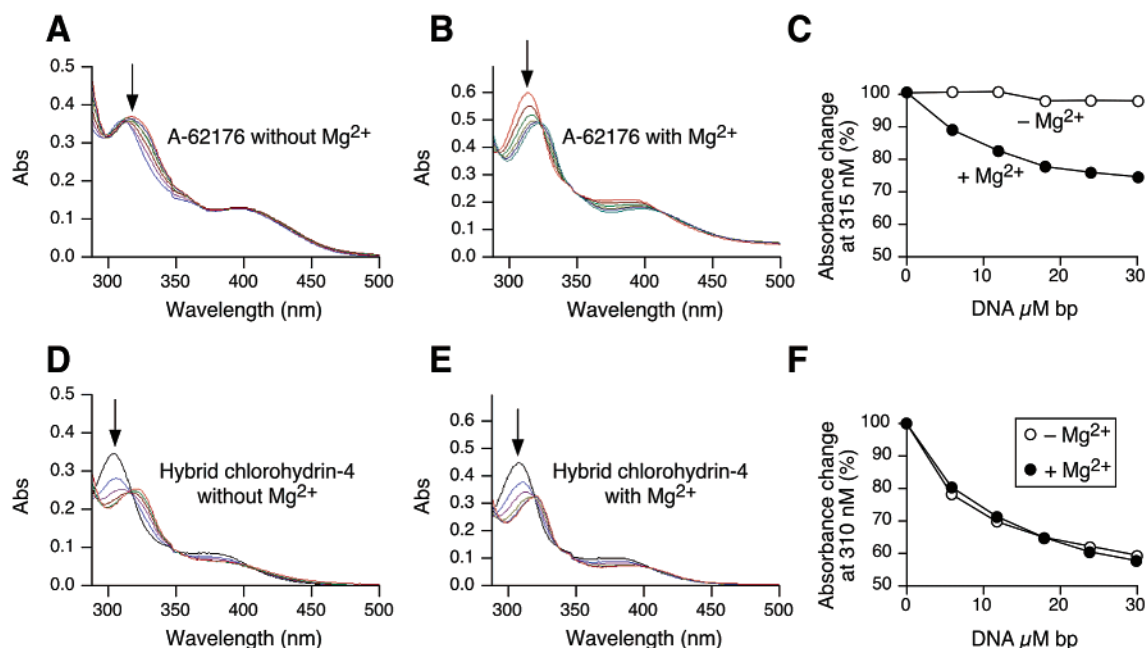


Figure 6. Effects of increasing DNA concentrations on the UV absorption of A-62176 and hybrid chlorohydrin-4 in the absence and presence of 10 mM Mg^{2+} . A-62176 was incubated with increasing concentrations of the 60-mer duplex DNA in the absence (A) and presence (B) of Mg^{2+} . The percent of absorbance changes of A-62176 at 315 nm as a function of increasing concentrations of DNA in the absence and presence of Mg^{2+} is shown in panel C. Hybrid chlorohydrin-4 was incubated with increasing concentrations of the 60-mer duplex DNA in the absence (D) and presence (E) of Mg^{2+} . The percent of absorbance changes of hybrid chlorohydrin-4 at 310 nm as a function of increasing concentrations of DNA in the absence and presence of Mg^{2+} is shown in panel F. The arrows indicate a change in the spectrum brought on by increased concentrations of DNA.

Table 2. Cytotoxicities of A-62176, Psorospermin, and the Hybrid Compounds against Various Cancer Cells

cell lines (origin)	IC ₅₀ (μM)			
	A-62176	psorospermin	hybrid epoxide-3	hybrid chlorohydrin-4
HT29 (colon)	0.45 ^a	1.11	0.14	0.09
DU145 (prostate)	0.47	0.21	0.08	0.03
Hela (cervix)	0.80	1.46	0.29	0.13
MCF7 (breast)	0.66	0.57	0.24	0.08
H522 (NSCLS)	0.30	0.77	0.07	0.02
8226 (myeloma)	0.27	0.29	0.09	0.05
8226/Dox40 (Dox-Re)	0.27	0.23	0.05	0.03
U937 (lymphoma)	0.31	0.27	0.03	0.02
Granta (lymphoma)	0.09	0.04	0.004	0.002
MiaPaCa (pancreas)	0.42	0.38	0.09	0.04

^a Each value is the average of four experiments.

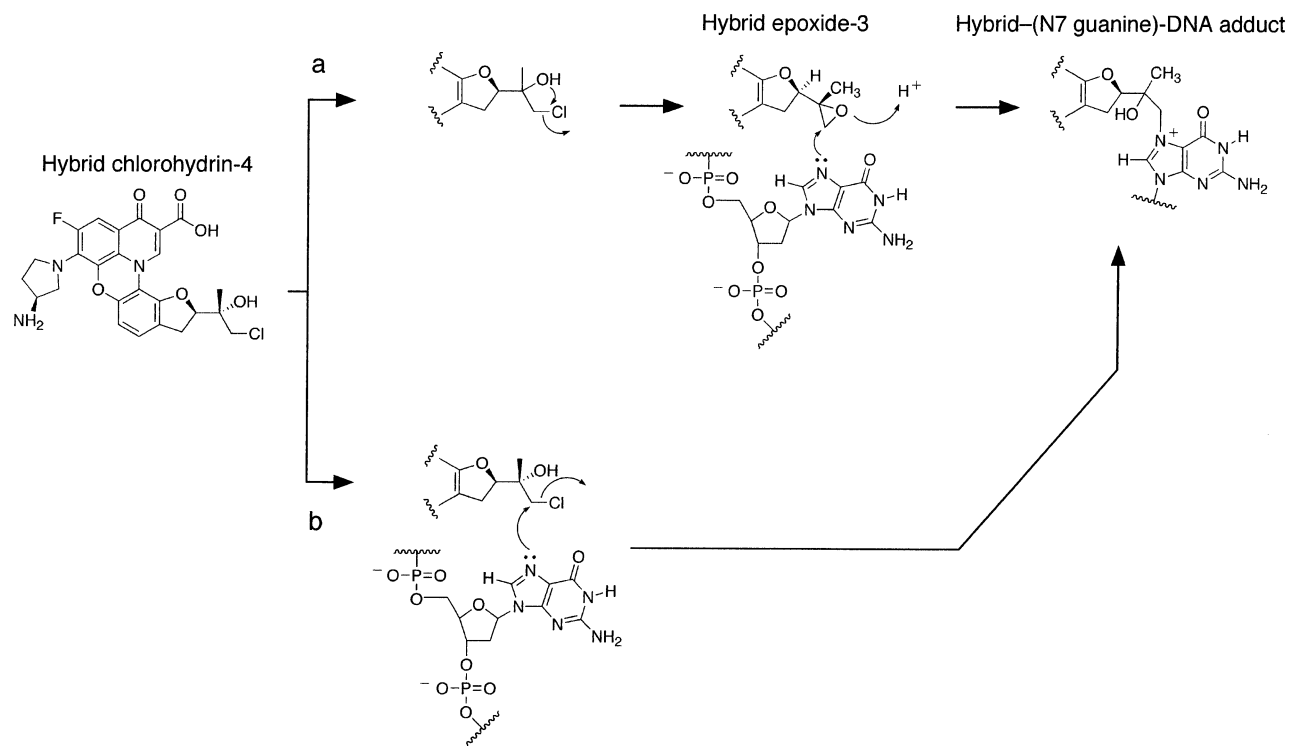


Figure 7. Proposed alternative activation mechanisms for hybrid chlorohydrin-4, leading to formation of the hybrid-DNA adduct inside cells. In pathway "a", hybrid epoxide-3 is an intermediate, while in pathway "b", alkylation takes place at the chlorohydrin level.

epoxide-3 shows stable binding with duplex DNA, and its reactive epoxide moiety is close to the nucleophilic N₇ of guanine, resulting in stronger DNA alkylating activity than psorospermin in the presence of topoisomerase II.

Hybrid chlorohydrin-4 was also designed and synthesized by modifying the functional epoxy group of hybrid epoxide-3 with chlorohydrin, with the aim of enhancing both nucleophilicity and accessibility to N₇ of guanine. Hybrid chlorohydrin-4 showed more potent cytotoxicity than hybrid epoxide-3 against various cancer cell lines. However, our initial assays for DNA alkylating activity at pH 7.6 showed that hybrid chlorohydrin-4 had no activity, a result that seemed to be at odds with our proposal that the cytotoxic effect of the hybrid compounds is primarily due to their DNA alkylating activity. It is likely that hybrid chlorohydrin-4 is converted into DNA-reactive intermediates inside cells, where nucleophilic displacement of the chloride can occur either by the adjacent hydroxyl group of the compounds, which would result in the formation of an epoxide ring,

or by N₇ of guanine directly attacking the chloride (Figure 7). The resulting covalent DNA adducts are similar to those for hybrid epoxide-3. To test this hypothesis, the hybrid compounds were analyzed for DNA alkylating activity at higher pH conditions, which are more favorable for nucleophilic displacement of the chloride. Under these conditions, the DNA alkylating activity of hybrid chlorohydrin-4 was significantly increased.

In conclusion, the structures of psorospermin and A-62176 were used as a basis for the rational design of novel DNA alkylating agents. Some of the more promising of these compounds were identified using molecular modeling, and these were synthesized and tested for their DNA alkylating activity under various conditions. The novel hybrid compounds showed enhanced DNA alkylating activities in the presence of topoisomerase II and exhibited significant activity *in vitro* against various tumor cell lines. However, the hybrid compounds may have lost some of the topoisomerase II and Mg²⁺ dependency for reaction with DNA that is associ-

ated with psorospermin and A-62176,^{6,21,22} most likely by the stable binding of hybrid compounds to DNA, even in the absence of topoisomerase II and Mg²⁺. Although additional studies are necessary to develop a deeper understanding of these preliminary results, they are very encouraging. These compounds are under further evaluation for in vivo activity.

Experimental Section

General Method for Chemistry. ¹H NMR spectra were taken on Bruker AMX 500 and 300 MHz instruments. Chemical shifts (δ) are in parts per million (ppm) relative to tetramethylsilane, and coupling constants (J value) are in hertz. Low-resolution and high-resolution mass spectral investigations were conducted by the Mass Spectroscopy Facility at the University of Arizona. The solvents and reactants were of the best commercial grade available and were used without further purification unless noted.

2,3-Dihydro-2-(2-isopropenyl)-6-hydroxy-7-nitrobenzofuran (1). To a solution of 2-nitroresorcinol (1.6 g, 10 mmol) in anhydrous toluene (40 mL), *n*-BuLi (10 mL, 1.6 M in hexane) was added under nitrogen. The mixture was stirred at room temperature (15 min), and then a solution of 2-methyl-*trans*-1,4-dibromo-2-butene (3.4 g, 10 mmol) in toluene (2 mL) was added by syringe under nitrogen. The resulting dark slurry was refluxed at 110 °C (22 h), saturated NH₄Cl (30 mL) was added to quench the reaction, and the residue was extracted with ether (100 mL). The organic layer was separated, washed with saturated NaCl (50 mL), and dried (Na₂SO₄). After removal of the solvent under reduced pressure, the residue was purified by silica gel column chromatography (10–30% EtOAc/hexane) to give 0.5 g (23%) of a dark-yellow semisolid compound: R_f = 0.54 (20% EtOAc/hexane); ¹H NMR (CDCl₃, 500 MHz) δ 1.79 (s, 3H), 3.03 (dd, J = 15.3, 8.7 Hz, 1H), 3.35 (dd, J = 15.3, 9.5 Hz, 1H), 4.98 (s, 1H), 5.14 (s, 1H), 5.46 (dd, J = 9.5, 8.7 Hz, 1H), 6.58 (d, J = 7.8 Hz, 1H), 7.26 (d, J = 7.8 Hz, 1H), 10.71 (s, 1H); MS (FAB) m/e 221 [M]⁺; M_r (FAB) 221.0690 [M]⁺ (calcd for C₁₁H₁₁NO₄ 221.0688).

A Mixture of 2,3-Dihydro-2(R)-(1,2(R)-dihydroxypropan-2-yl)-6-hydroxy-7-nitrobenzofuran and 2,3-Dihydro-2(S)-(1,2(S)-dihydroxypropan-2-yl)-6-hydroxy-7-nitrobenzofuran (2) and a Mixture of 2,3-Dihydro-2(S)-(1,2(R)-dihydroxypropan-2-yl)-6-hydroxy-7-nitrobenzofuran and 2,3-Dihydro-2(R)-(1,2(S)-dihydroxypropan-2-yl)-6-hydroxy-7-nitrobenzofuran (3). To a solution of 4-methylmorpholine *N*-oxide (0.5 g, 4.3 mmol) and OsO₄ (catalytic amount) in H₂O/acetone (1:1, 2 mL) was added compound 1 (0.8 g, 3.6 mmol) in CHCl₃ (2.5 mL). The mixture was stirred (2 h) and quenched with saturated NaHSO₃ (4 mL). After being stirred (10 min), the reaction mixture was extracted with EtOAc (20 mL). The organic layer was separated, washed with saturated NaCl, and dried (Na₂SO₄). Solvent was removed under reduced pressure and the residue was purified by PTLC (5% MeOH/CHCl₃) to give 0.4 g (41%) of 2 and 0.1 g (11%) of 3.

Compound 2: R_f = 0.58 (10% MeOH/CHCl₃); ¹H NMR (CDCl₃, 500 MHz) δ 1.21 (s, 3H), 3.19 (dd, J = 15.5, 9.0 Hz, 1H), 3.35 (dd, J = 15.5, 8.0 Hz, 1H), 3.57 (d, J = 11.1 Hz, 1H), 3.82 (d, J = 11.1 Hz, 1H), 5.06 (dd, J = 9.0, 8.0 Hz, 1H), 6.58 (d, J = 8.8 Hz, 1H), 7.27 (d, J = 8.8 Hz, 1H), 10.59 (s, 1H); MS (FAB) m/e 255 [M]⁺; M_r (FAB) 255.0746 [M]⁺ (calcd for C₁₁H₁₃NO₆ 255.0743).

Compound 3: R_f = 0.67 (10% MeOH/CHCl₃); ¹H NMR (CDCl₃, 500 MHz) δ 1.14 (s, 3H), 3.16 (dd, J = 14.8, 9.5 Hz, 1H), 3.36 (dd, J = 14.8, 8.5 Hz, 1H), 3.57 (d, J = 11.8 Hz, 1H), 3.99 (d, J = 11.8 Hz, 1H), 5.03 (dd, J = 9.5, 8.5 Hz, 1H), 6.60 (d, J = 8.3 Hz, 1H), 7.28 (d, J = 8.3 Hz, 1H), 10.58 (s, 1H); MS (FAB) m/e 255 [M]⁺; M_r (FAB) 255.0746 [M]⁺ (calcd for C₁₁H₁₃NO₆ 255.0743).

7-Amino-2,3-dihydro-2(R)-(1,2(R)-dihydroxypropan-2-yl)-6-hydroxybenzofuran (4). Compound 2 (0.13 g, 0.5 mmol) and 10% Pd/C (17 mg) were placed in a reaction bottle, and MeOH (60 mL) was added. The mixture was shaken under H₂ (65 mmHg) overnight and filtered using Celite. The solvent

was removed in vacuo to afford 0.1 g (93%) of 4 as a gray solid: ¹H NMR (CD₃OD, 300 MHz) δ 1.30 (s, 3H), 3.08 (dd, J = 12.0, 9.0 Hz, 1H), 3.20 (dd, J = 12.0, 8.0 Hz, 1H), 3.52 (d, J = 11.3 Hz, 1H), 3.64 (d, J = 11.3 Hz, 1H), 4.82 (dd, J = 9.0, 8.0 Hz, 1H), 6.27 (d, J = 7.9 Hz, 1H), 6.46 (d, J = 7.9 Hz, 1H); MS (FAB) m/e 225 [M]⁺; M_r (FAB) 225.1009 [M]⁺ (calcd for C₁₁H₁₅NO₄ 225.1001).

Enantiomeric Mixture of Ethyl 3-[2,3-Dihydro-2(R)-(1,2(R)-dihydroxypropan-2-yl)-6-hydroxybenzofuranyl-7-amino]-2-(2,3,4,5-tetrafluorobenzoyl)-2-propenoate and Ethyl 3-[2,3-Dihydro-2(S)-(1,2(S)-dihydroxypropan-2-yl)-6-hydroxybenzofuranyl-7-amino]-2-(2,3,4,5-tetrafluorobenzoyl)-2-propenoate (5). A solution of ethyl 2,3,4,5-tetrafluorobenzoylacetate (124 mg, 0.5 mmol) in triethyl orthoformate (0.25 mL, 1.5 mmol) and acetic anhydride (0.4 mL, 4.2 mmol) was stirred at 130 °C (4 h). The solvent was removed in vacuo. The oil residue was dissolved in CHCl₃ (3 mL), and compound 4 (105 mg, 0.5 mmol) in CHCl₃ and pyridine (4:1, 1 mL) was added. After the mixture was stirred at room temperature (17 h), the solvent was removed under reduced pressure. The residue was purified by silica gel column chromatography (5–10% MeOH/CHCl₃) to give 200 mg (86%) of 5 as an orange solid: R_f = 0.60 (10% MeOH/CHCl₃); ¹H NMR (CDCl₃/CD₃OD (2:1), 500 MHz) δ 0.88 (t, J = 7.0 Hz, 3H), 0.98 (s, 3H), 2.97 (dd, J = 14.8, 9.0 Hz, 1H), 3.10 (dd, J = 14.8, 8.0 Hz, 1H), 3.39 (d, J = 10.8 Hz, 1H), 3.55 (d, J = 10.8 Hz, 1H), 3.93 (q, J = 7.0 Hz, 2H), 4.82 (dd, J = 9.0, 8.0 Hz, 1H), 6.25 (d, J = 7.8 Hz, 1H), 6.65 (d, J = 7.8 Hz, 1H), 6.90 (br s, 1H), 9.11 (s, 1H); MS (FAB) m/e 499 [M]⁺; M_r (FAB) 499.1234 [M]⁺ (calcd for C₂₃H₂₁NO₇F₄ 499.1254).

Enantiomeric Mixture of Ethyl 1,2-Difluoro-4-oxo-4H-pyrido[3,2,1-*k*]-2(R)-((1,2(R)-dihydroxypropan-2-yl)-1,2-dihydrofurano)[*h*]phenoxazine-5-carboxylate and Ethyl 1,2-Difluoro-4-oxo-4H-pyrido[3,2,1-*k*]-2(S)-((1,2(S)-dihydroxypropan-2-yl)-1,2-dihydrofurano)[*h*]phenoxazine-5-carboxylate (6). Compound 5 (138 mg, 0.28 mmol) and NaHCO₃ (116 mg, 1.38 mmol) were placed in DMF (4 mL) under nitrogen, and the mixture was refluxed at 110 °C (2 h). Solvent was removed under reduced pressure, and the residue was dissolved using both CHCl₃ and water. Undissolved material was filtered, and the organic layer was separated. After the solvent was removed, the residue was purified by silica gel column chromatography (10% MeOH/CHCl₃) to give 100 mg (79%) of 6 as a light-gray solid: R_f = 0.69 (10% MeOH/CHCl₃); ¹H NMR (CDCl₃, 500 MHz) δ 1.40 (t, J = 7.1 Hz, 3H), 1.43 (s, 3H), 3.19 (dd, J = 15.7, 9.4 Hz, 1H), 3.43 (dd, J = 15.7, 9.4 Hz, 1H), 3.60 (d, J = 11.3 Hz, 1H), 3.86 (d, J = 11.3 Hz, 1H), 4.38 (q, J = 7.1 Hz, 2H), 5.13 (dd, J = 9.4, 9.4 Hz, 1H), 6.60 (d, J = 8.1 Hz, 1H), 7.02 (d, J = 8.1 Hz, 1H), 7.43 (dd, J = 9.9, 5.9 Hz, 1H), 9.76 (s, 1H); MS (FAB) m/e 460 [M + H]⁺; M_r (FAB) 460.1203 [M + H]⁺ (calcd for C₂₃H₂₀NO₇F₂ 460.1208).

Diastereomeric Mixture of Ethyl 1-(3(S)-*tert*-Butoxycarbonylamino)pyrrolidin-1-yl)-2-fluoro-4-oxo-4H-pyrido[3,2,1-*k*]-2(R)-((1,2(R)-dihydroxypropan-2-yl)-1,2-dihydrofurano)[*h*]phenoxazine-5-carboxylate and Ethyl 1-(3(S)-*tert*-Butoxycarbonylamino)pyrrolidin-1-yl)-2-fluoro-4-oxo-4H-pyrido[3,2,1-*k*]-2(S)-((1,2(S)-dihydroxypropan-2-yl)-1,2-dihydrofurano)[*h*]phenoxazine-5-carboxylate (7). Compound 6 (90 mg, 0.20 mmol) and 3(S)-*tert*-butoxycarbonylamino)pyrrolidine (109 mg, 0.59 mmol) were dissolved in anhydrous pyridine (5 mL), and the mixture was stirred under nitrogen at 110 °C (56 h). The solvent was removed under reduced pressure, and the residue was purified by PTLC (5% MeOH/CHCl₃) to give 80 mg (65%) of 7 as a solid: R_f = 0.60 (10% MeOH/CHCl₃); ¹H NMR (CDCl₃, 500 MHz) δ 1.36 (1.37) (t, J = 7.0 Hz, 3H), 1.50 (s, 12H), 1.92–1.96 (m, 1H), 2.19–2.23 (m, 1H), 3.10 (dd, J = 14.5, 9.1 Hz, 1H), 3.41 (dd, J = 14.5, 11.0 Hz, 1H), 3.54 (d, J = 11.6 Hz, 1H), 3.62–3.73 (m, 4H), 3.83–3.89 (m, 1H), 4.22–4.33 (m, 3H), 5.10 (dd, J = 11.0, 9.1 Hz, 1H), 6.30 (6.31) (d, J = 7.8 Hz, 1H), 6.89 (d, J = 7.8 Hz, 1H), 7.13–7.18 (m, 1H), 9.40 (9.44) (s, 1H); MS (FAB) m/e 625 [M]⁺; M_r (FAB) 625.2433 [M]⁺ (calcd for C₃₂H₃₆N₃O₉F 625.2436).

Diastereomeric Mixture of 1-(3(*S*)-*tert*-Butoxycarbonylamino)pyrrolidin-1-yl)-2-fluoro-4-oxo-4*H*-pyrido[3,2,1-*kl*]-2(*R*)-((1,2(*R*)-dihydroxypropan-2-yl)-1,2-dihydrofurano)[*h*]phenoxazine-5-carboxylic Acid and 1-(3(*S*)-*tert*-Butoxycarbonylamino)pyrrolidin-1-yl)-2-fluoro-4-oxo-4*H*-pyrido[3,2,1-*kl*]-2(*S*)-((1,2(*S*)-dihydroxypropan-2-yl)-1,2-dihydrofurano)[*h*]phenoxazine-5-carboxylic Acid (8). Compound 7 (70 mg, 0.1 mmol) was mixed with ethanol (1 mL) and 1 N KOH (0.5 mL). This mixture was refluxed at 80 °C (1 h) and cooled to room temperature. The reaction mixture was acidified with 2 N HCl (0.5 mL). The solid that precipitated was isolated by filtration, washed with water, and dried in vacuo to give 58 mg (88%) of **8** as an orange solid: $R_f = 0.73$ (30% MeOH/CHCl₃); ¹H NMR (CDCl₃/CD₃OD (3:2), 500 MHz) δ 1.07 (s, 9H), 1.63–1.65 (m, 1H), 1.87–1.91 (m, 1H), 2.90 (dd, $J = 15.8, 9.4$ Hz, 1H), 3.05 (dd, $J = 15.8, 9.4$ Hz, 1H), 3.24 (d, $J = 11.3$ Hz, 1H), 3.26–3.29 (m, 1H), 3.35 (d, $J = 11.3$ Hz, 1H), 3.47–3.50 (m, 1H), 3.57–3.63 (m, 2H), 3.88–3.92 (m, 1H), 4.79 (dd, $J = 9.4, 9.4$ Hz, 1H), 6.30 (6.31) (d, $J = 8.0$ Hz, 1H), 6.76 (d, $J = 8.0$ Hz, 1H), 7.16 (7.17) (d, $J = 13.5$ Hz, 1H), 9.61 (9.62) (s, 1H); MS (FAB) m/e 598 [M + H]⁺; M_r (FAB) 598.2214 [M]⁺ (calcd for C₃₀H₃₃N₃O₉F 598.1976).

Diastereomeric Mixture of 1-(3(*S*)-*tert*-Butoxycarbonylamino)pyrrolidin-1-yl)-2-fluoro-4-oxo-4*H*-pyrido[3,2,1-*kl*]-2(*R*)-((2(*R*)-hydroxy-1-methanesulfonyloxypropan-2-yl)-1,2-dihydrofurano)[*h*]phenoxazine-5-carboxylic Acid and 1-(3(*S*)-*tert*-Butoxycarbonylamino)pyrrolidin-1-yl)-2-fluoro-4-oxo-4*H*-pyrido[3,2,1-*kl*]-2(*S*)-((2(*S*)-hydroxy-1-methanesulfonyloxypropan-2-yl)-1,2-dihydrofurano)[*h*]phenoxazine-5-carboxylic Acid (9). To an anhydrous pyridine (5 mL) solution of compound **8** (50 mg, 0.09 mmol), methanesulfonyl chloride (33 μ L, 0.42 mmol) was added dropwise in an ice bath. The reaction mixture was stirred at 0 °C (30 min), and water was added. The solid precipitate was extracted with CHCl₃, and the organic layer was washed with water and brine successively. Solvent was removed in vacuo to give 53 mg (97%) of **9** as a solid: $R_f = 0.60$ (10% MeOH/CHCl₃); ¹H NMR (CDCl₃, 500 MHz) δ 1.48 (s, 9H), 1.53 (s, 3H), 1.94–1.97 (m, 1H), 2.17–2.22 (m, 1H), 3.14–3.20 (m, 1H), 3.18 (s, 3H), 3.43–3.46 (m, 1H), 3.54–3.59 (m, 1H), 3.70–3.74 (m, 1H), 3.88–3.92 (m, 2H), 4.10–4.28 (m, 3H), 5.00–5.05 (m, 1H), 6.54 (d, $J = 7.4$ Hz, 1H), 7.03 (d, $J = 7.4$ Hz, 1H), 7.28 (d, $J = 13.2$ Hz, 1H), 9.69 (s, 1H); MS (FAB) m/e 676 [M + H]⁺; M_r (FAB) 676.1992 [M]⁺ (calcd for C₃₁H₃₅N₃O₁₁FS 676.1976).

Diastereomeric Mixture of 1-(3(*S*)-Aminopyrrolidin-1-yl)-2-fluoro-4-oxo-4*H*-pyrido[3,2,1-*kl*]-2(*R*)-(1(*R*)-methyloxyanyl)-1,2-dihydrofurano)[*h*]phenoxazine-5-carboxylic Acid and 1-(3(*S*)-Aminopyrrolidin-1-yl)-2-fluoro-4-oxo-4*H*-pyrido[3,2,1-*kl*]-2(*S*)-(1(*S*)-methyloxyanyl)-1,2-dihydrofurano)[*h*]phenoxazine-5-carboxylic Acid (Hybrid Epoxide-3). Compound **9** (18 mg, 0.03 mmol) was dissolved in a mixture of 3 N HCl and ethyl acetate (0.5 mL), and the reaction solution was stirred at room temperature (10 min). The solvent was removed under reduced pressure, and the residue was dissolved in ether (5 mL) and sonicated (2 \times 2 min). The organic layer was decanted, and the residue was redissolved in methanol (3 mL) and concentrated in vacuo to 14 mg of a solid. This compound was mixed with *t*-BuOK (25.6 mg, 0.22 mmol) in *t*-butanol (8 mL), and the reaction mixture was stirred at 40 °C (2 h). The reaction mixture was partitioned between CHCl₃ and water (6 mL, 2:1). The aqueous layer was extracted with CHCl₃ (5 mL), and the combined organic layer was washed with saturated NaCl and dried with Na₂SO₄. The solvent was removed in vacuo to give 4 mg (32%) of hybrid epoxide-3 as an orange solid: ¹H NMR (CDCl₃, 300 MHz) δ 1.67 (s, 3H), 2.15–2.21 (m, 1H), 2.30–2.35 (m, 1H), 2.77 (d, $J = 4.1, 1H$), 2.80 (d, $J = 4.1, 1H$), 3.01–3.12 (m, 2H), 3.45–3.52 (m, 1H), 3.66–3.94 (m, 2H), 3.94–4.06 (m, 2H), 5.16 (dd, $J = 9.3, 8.7$ Hz, 1H), 6.59 (d, $J = 8.1$ Hz, 1H), 7.00 (d, $J = 8.1$ Hz, 1H), 7.57 (d, $J = 11.7$ Hz, 1H), 9.93 (9.94) (s, 1H); MS (MALDI-TOF) M_r 480.1575 [M + H]⁺ (calcd for C₂₅H₂₃N₃O₆F 480.1571).

Diastereomeric Mixture of 1-(3(*S*)-*tert*-Butoxycarbonylamino)pyrrolidin-1-yl)-2-fluoro-4-oxo-4*H*-pyrido[3,2,1-

***kl*]-2(*R*)-(1(*R*)-methyloxyanyl)-1,2-dihydrofurano)[*h*]phenoxazine-5-carboxylic Acid and 1-(3(*S*)-*tert*-Butoxycarbonylamino)pyrrolidin-1-yl)-2-fluoro-4-oxo-4*H*-pyrido[3,2,1-*kl*]-2(*S*)-(1(*S*)-methyloxyanyl)-1,2-dihydrofurano)[*h*]phenoxazine-5-carboxylic Acid (10).** To an acetone (4 mL) solution of compound **9** (18 mg, 0.03 mmol), 18-crown-6 (7 mg, 0.03 mmol) and K₂CO₃ (37 mg, 0.27 mmol) were added. The reaction mixture was stirred overnight and extracted with CHCl₃. The organic layer was washed with dilute HCl and saturated NaCl aqueous solution successively. After removal of the solvent under reduced pressure, the residue was purified by PTLC (8% MeOH/CHCl₃) to afford 11 mg (70%) of **10** as a solid: $R_f = 0.68$ (10% MeOH/CHCl₃); ¹H NMR (CDCl₃, 500 MHz) δ 1.47 (s, 9H), 1.63 (1.65) (s, 3H), 1.93–1.96 (m, 1H), 2.17–2.22 (m, 1H), 2.75–2.77 (m, 1H), 2.78–2.80 (m, 1H), 3.00 (dd, $J = 15.1, 8.3$ Hz, 1H), 3.08 (dd, $J = 15.1, 8.6$ Hz, 1H), 3.53–3.57 (m, 1H), 3.68–3.71 (m, 1H), 3.86–3.91 (m, 1H), 3.94–3.98 (m, 1H), 4.31–4.37 (m, 1H), 4.90 (br s, 1H), 5.15 (dd, $J = 8.6, 8.3$ Hz, 1H), 6.59 (d, $J = 8.0$ Hz, 1H), 7.00 (d, $J = 8.0$ Hz, 1H), 7.58 (7.60) (d, $J = 13.5$ Hz, 1H), 9.95 (9.97) (s, 1H); MS (FAB) m/e 580 [M + H]⁺; M_r (FAB) 580.2096 [M]⁺ (calcd for C₃₀H₃₁N₃O₁₈F 580.2095).

Diastereomeric Mixture of 1-(3(*S*)-Aminopyrrolidin-1-yl)-2-fluoro-4-oxo-4*H*-pyrido[3,2,1-*kl*]-2(*R*)-((2(*R*)-hydroxy-1-chloropropan-2-yl)-1,2-dihydrofurano)[*h*]phenoxazine-5-carboxylic Acid Hydrogen Chloride and 1-(3(*S*)-Aminopyrrolidin-1-yl)-2-fluoro-4-oxo-4*H*-pyrido[3,2,1-*kl*]-2(*S*)-((2(*S*)-hydroxy-1-chloropropan-2-yl)-1,2-dihydrofurano)[*h*]phenoxazine-5-carboxylic Acid Hydrogen Chloride (Hybrid Chlorohydrin-4). Compound **10** (7 mg, 0.01 mmol) was dissolved in 1 N HCl and aqueous ethyl acetate (1.0 mL), and the reaction solution was stirred at room temperature (10 min). The solvent was removed under reduced pressure, and the residue was dissolved in ether (5 mL) and sonicated (2 min \times 2). The organic layer was decanted, and the residue was redissolved in methanol (3 mL) and concentrated in vacuo to afford 6.5 mg (90%) of hybrid chlorohydrin-4 as an orange solid: ¹H NMR (CD₃OD, 300 MHz) δ 1.47 (s, 3H), 2.13–2.19 (m, 1H), 2.44–2.53 (m, 1H), 3.11–3.30 (m, 2H), 3.67–3.85 (m, 4H), 3.90–4.05 (m, 1H), 4.80–4.86 (m, 1H), 5.11–5.22 (m, 1H), 6.70–6.76 (m, 1H), 7.10–7.18 (m, 1H), 7.42–7.50 (m, 1H), 9.66 (s, 1H); MS (ESI): m/e 516 [M + H]⁺; M_r (MALDI-TOF) 516.1314 [M + H]⁺ (calcd for C₂₅H₂₄N₃O₆FCI 516.1337).

Materials for Biochemistry. Compound solutions were prepared as 1 mM stock solutions in dimethyl sulfoxide and stored at –20 °C. Psorospermin was a generous gift from John M. Cassidy (The Ohio State University). These stock solutions were diluted to working concentrations in distilled water immediately before use. Electrophoretic reagents (acrylamide/bisacrylamide solutions and ammonium persulfate) were purchased from BioRad, and *N,N,N,N*-tetramethylethylenediamine was purchased from Fisher. T4 polynucleotide kinase, Taq DNA polymerase, and human topoisomerase II were purchased from New England Biolabs, Promega, and TopoGen, respectively. [γ -³²P]ATP was purchased from NEN Dupont.

Preparation and End-Labeling of Oligonucleotides. Oligonucleotides were synthesized on an Expedite 8909 nucleic acid synthesis system (PerSeptive Biosystems, Framingham, MA) using the phosphoramidite method. The oligonucleotides were eluted out of the column using aqueous ammonia and deprotected by heating at 55 °C overnight, followed by 15% denaturing polyacrylamide gel purification. The 5'-end-labeled single-strand oligonucleotide was obtained by incubating the oligomer with T4 polynucleotide kinase and [γ -³²P]ATP for 1 h at 37 °C. Labeled DNA was purified with a Bio-Spin 6 chromatography column (BioRad) after inactivating the kinase by heating for 8 min at 70 °C.

DNA Alkylation Assay. Oligomers A1 (d[CGCCGAAAC-AAGCGCTCATGAGCCCCGTATCAATGTATACGAGC-CGGATCTTCCCCATCG]) and A2 (d[CGATGGGGAAGAT-CGGCTCGTATACATTGATACGGGGCTCATGAGCGCT-TTTTCGGCG]) were synthesized as mentioned above. The

5'-end-labeled A1 was annealed with the complementary strand (A2) by heating to 95 °C and slowly cooled to room temperature. Labeled double-stranded DNA was purified on an 8% native polyacrylamide gel. DNA was incubated with 20 units of human topoisomerase II in 20 μ L of reaction buffer (30 mM Tris-HCl, pH 7.6, 3 mM ATP, 15 mM β -mercaptoethanol, 8 mM MgCl₂, 60 mM NaCl) at 30 °C for 20 min in the presence of various concentrations of compounds.³⁰ The reaction was terminated by adding 5 μ g of calf thymus DNA, followed by phenol/chloroform extraction and ethanol precipitation. DNA samples were then subjected to piperidine treatment and 12% denaturing polyacrylamide gel electrophoresis. For the experiment with higher pH conditions, 10 mM glycine/NaOH buffers were used.

Topoisomerase II Mediated Cleavage Reaction. The topoisomerase II mediated cleavage reaction was carried out essentially as described before for the DNA alkylation assay, with the following modifications. DNA was incubated with 20 units of human topoisomerase II in 20 μ L of reaction buffer (30 mM Tris-HCl, pH 7.6, 3 mM ATP, 15 mM β -mercaptoethanol, 8 mM MgCl₂, 60 mM NaCl) at 30 °C for 10 min in the presence of various concentrations of compounds.³⁰ Reactions were terminated by adding SDS to 1% of the final concentration, and topoisomerase II was removed by proteinase K digestion (100 μ g/mL) at 42 °C for 1 h, followed by phenol/chloroform extraction and ethanol precipitation. Samples were loaded onto a 12% denaturing sequencing gel.

Imaging and Quantification. The dried gels were exposed on a phosphor screen. Imaging and quantification were performed using a PhosphorImager (Storm 820) and ImageQuant 5.1 software from Molecular Dynamics.

Cytotoxicity Assay. Cancer cells were purchased from the American Tissue Culture Collection (Rockville, MD) and cultured according to the supplier's instructions. Exponentially growing cells ((1–2) \times 10³ cells) in 0.1 mL of medium were seeded on day 0 in a 96-well microtiter plate. On day 1, 0.1 mL aliquots of medium containing graded concentrations of compound were added to the cell plates. On day 4, the cell cultures were incubated with 50 μ L of 3-(4,5-dimethylthiazol-2-yl)-2,5-diphenyltetrazolium bromide (1 mg/mL in Dulbecco's phosphate buffered saline) for 4 h at 37 °C. The resulting formazan precipitate was solubilized with 200 μ L of 0.04 M HCl in isopropyl alcohol. For determination of the IC₅₀ values, the absorbance readings at 570 nm were fitted to the four-parameter logistic equation.

Molecular Modeling. Molecular graphics, structural manipulations, energy minimization, molecular docking, and MD simulations were carried out on a Silicon Graphics Indigo2 workstation using the Biopolymer, Discover_3, CFF, Amber, and Affinity modules^{31–35} within the Insight II software (version 2000.1).³⁶

The high-resolution crystal structure (1.50 Å) coordinates published for doxorubicin bound to d[(C1G2T3A4C5G6)/(C7G8T9A10C11G12)] duplex DNA (PDB entry 2DES)²⁴ were used as a template to build the molecular model of the psorospermin–DNA and quinobenzoxazine–DNA complexes. In the first step, doxorubicin and one Mg²⁺ were retained at the d[(C5G6)/(C7G8)] region, while the second molecule of doxorubicin at the d[(C1.G2)/(C11.G12)] region was removed. The hydrogens in this structure were supplied by the Biopolymer module, and the positions were refined by minimizing the system using the Amber force field³³ until convergence was reached, while constraining the position of heavy atoms. To retain the charge neutrality of the phosphate backbone, two sodium ions found in the crystal structure were retained, and additional sodium ions were added using option counterions. The well-documented multistage minimization procedure³⁶ was used to attenuate any internal strains in the model of DNA at its current level of refinement, in which atoms were unconstrained in stages to remove strained interactions. The phosphate backbone atoms of the model were constrained to remain as close as possible to the corresponding phosphate backbone atoms of the crystal structure. The calculations were performed using a Polak–Ribiere conjugate gradient algorithm

for 2 \times 2000 steps of minimization. The solvent molecules were dealt with implicitly using a distance-dependent dielectric constant function ($\epsilon = 4r_{ij}$),^{37,38} and the charges were calculated using the Gasteiger method.³⁹ The coordinates from this structure were further used for SA docking, MD simulations, and complex formation.

Psorospermin, A-62176, and the hybrid compounds (shown in Table 1) were empirically built using Insight II. The charges for the ligands were calculated by semiempirical MOPAC using Insight II.³⁶ Systematic conformational searches were performed on each of the minimized ligands using 10 ps MD simulations at 300 K. For docking with psorospermin and A-62176, the position of the anthracycline moiety of doxorubicin was retained from the crystal structure, i.e., from step 1 before. A-62176 was inserted into the preformed intercalation binding site d[(C5G6)/(C7G8)] in which the fluorine-substituted aromatic ring and the 1,4-dihydroquinoline ring of A-62176 were superimposed on the C/D rings of the doxorubicin crystal structure.²⁴ The stacking pattern was determined by examining the relative orientation of the 2-oxiranyl, 6-(3-aminopyrrolidine), and carboxyl groups with the bases at d[(C5G6)/(C7G8)]. In one orientation, the 2-oxiranyl ring of A-62176 is sandwiched between the C5 and G6 bases and the carbonyl function is positioned close to the Mg²⁺ ion. Similarly, the 6-(3-aminopyrrolidine) ring of A-62176 is oriented into the minor groove, and this orientation allows the formation of a favorable Mg²⁺ ion coordination with the sp² oxygens of the carbonyl and carboxyl functional groups. This position was used for field fit alignments. In subsequent experiments, each of the other ligands was similarly docked manually, using Affinity, into the active site pocket of d[(C5G6)/(C7G8)] with an equivalent position and orientation. The heavy atoms from the crystal structure template were used as sphere centers in the input to the docking procedure. To clarify the orientation of these ligands in the intercalation site, the electrostatic potential at the van der Waals surface was determined using solvent surface calculations. The orientations with the lowest intermolecular potential energies were calculated. To explore the interaction of the ligands in the recognition pocket, Affinity SA docking of the complex formation was carried out without constraints to let each of the DNA–ligand complex systems evolve freely. Affinity is an energy-based method that uses a Monte Carlo procedure in conjunction with simulated annealing and minimization. Affinity allows predefined atoms of the ligand and the intercalation site to relax during docking. The nonbonded cell multipole method³⁴ was used for SA docking with input from CFF energy parameters. Docking simulations were performed at 500 K with 100 fs/stage (total of 50 stages), quenching the system to a final temperature of 300 K. The whole complex structure was energy-minimized using 1000 steps. This provided 20 structures from SA docking, and the conformers generated were clustered according to root-mean-square deviation. To ensure the stability of the models, the complex structures obtained from Affinity SA docking were hydrated with a 5 Å TIP3 water shell,⁴⁰ added by using the Soak assembly function of Insight II, which resulted in 1694 water molecules.

Molecular dynamics simulations were carried out using the Verlet method,³⁶ and the *NVE* ensemble was used in all calculations. During MD simulations, the Rattle_Bond method⁴¹ was employed with time steps of 2 fs. The equilibration phase was 100 ps, and the second phase was for an additional 100 ps. For all calculations, a temperature of 300 K was used. The Amber force field parameters were used in all MD calculations, employing a 20 Å cutoff distance for the treatment of electrostatic terms and a 10 Å cutoff distance for the treatment of all other nonbonded interactions. Molecular dynamics simulations were carried out only in the regions located around both the ligand and the d[(C5G6)/(C7G8)] step of DNA, keeping all other residues and water molecules in their initial positions. Within the intercalation site (i.e., d[(C5G6)/(C7G8)]), the bases were freed from restraints during all simulations, and the water molecules located within 15 Å had a quadratic restraint of 5 kcal/(Å²·mol). The models obtained after MD simulations

were minimized, using the same restraints as previously described, on the intercalation site by 1000 steps of conjugate gradient algorithm until the maximum derivative values were less than 0.01 kcal/mol. A comparison of the lowest global trajectory structures from the last run of SA docking and MD simulations in explicit solvent gave a root-mean-square deviation value of 0.4 Å for the ligand binding intercalation site and 0.6 Å for the overall structure. The obtained lowest global trajectory structure from the MD simulations was used for computing the intermolecular binding energies^{42,43} and are summarized in Table 1.

UV Spectrophotometric Assay. Absorbance spectra were recorded as described previously²¹ using a Cary UV-visible spectrophotometer. Sequential aliquots of DNA solution containing A-62176 and hybrid chlorohydrin-4 at a concentration of 20 μM were added to 20 μM drug solution containing 10 mM Tris buffer (pH 7.6) with or without 10 mM MgCl₂ in a 1 cm cuvette. The total drug concentration was thus maintained at a constant value. After the addition of each aliquot, the absorption spectrum (290–500 nm) was recorded.

Acknowledgment. This research was supported by the National Institutes of Health (Grants CA88310 and CA49751). We thank Dr. John M. Cassady (The Ohio State University) for providing the psorospermin and Dr. David Bishop for preparing, proofreading, and editing the final version of the manuscript and figures.

References

- Cassady, J. M.; Baird, W. M.; Chang, C.-J. Natural products as a source of potential cancer chemotherapeutic and chemopreventive agents. *J. Nat. Prod.* **1990**, *53*, 23–41.
- Kupchan, S. M.; Streelman, D. R.; Sneden, A. T. Psorospermin, a new antileukemic xanthone from *Psorospermum febrifugum*. *J. Nat. Prod.* **1980**, *43*, 296–301.
- Hansen, M.; Hurley, L. H. Pluramycins. Old drugs having modern friends in structural biology. *Acc. Chem. Res.* **1996**, *29*, 249–258.
- Hansen, M.; Yun, S.; Hurley, L. H. Hedamycin intercalates the DNA helix and, through carbohydrate-mediated recognition in the minor groove, directs N7-alkylation of guanine in the major groove in a sequence-specific manner. *Chem. Biol.* **1995**, *2*, 229–240.
- Hansen, M.; Lee, S.-J.; Cassady, J. M.; Hurley, L. H. Molecular details of the structure of a psorospermin–DNA covalent/intercalation complex and associated DNA sequence selectivity. *J. Am. Chem. Soc.* **1996**, *118*, 5553–5561.
- Kwok, Y.; Zeng, Q.; Hurley, L. H. Topoisomerase II-mediated site-directed alkylation of DNA by psorospermin and its use in mapping other topoisomerase II poison binding sites. *Proc. Natl. Acad. Sci. U.S.A.* **1998**, *95*, 13531–13536.
- Wang, J. C. Cellular roles of DNA topoisomerases: a molecular perspective. *Nat. Rev. Mol. Cell Biol.* **2002**, *6*, 430–440.
- Watt, P. M.; Hickson, I. D. Structure and function of type II DNA topoisomerases. *Biochem. J.* **1994**, *303*, 681–695.
- Nitiss, J. L. Investigating the biological functions of DNA topoisomerases in eukaryotic cells. *Biochim. Biophys. Acta* **1998**, *1400*, 63–81.
- Kellner, U.; Sehested, M.; Jensen, P. B.; Gieseler, F.; Rudolph, P. Culprit and victim—DNA topoisomerase II. *Lancet Oncol.* **2002**, *4*, 235–243.
- Pommier, Y. In *Cancer Therapeutics: Experimental and Clinical Agents*; Teicher, B. A., Ed.; Humana Press: Totowa, NJ, 1997; pp 153–174.
- Pommier, Y. DNA topoisomerase I and II in cancer chemotherapy: update and perspectives. *Cancer Chemother. Pharmacol.* **1993**, *32*, 103–108.
- Corbett, A. H.; Osheroff, N. When good enzymes go bad: conversion of topoisomerase II to a cellular toxin by antineoplastic drugs. *Chem. Res. Toxicol.* **1993**, *6*, 585–597.
- Osheroff, N.; Corbett, A. H.; Robinson, M. J. Mechanism of action of topoisomerase II-targeted antineoplastic drugs. *Adv. Pharmacol.* **1994**, *29B*, 105–126.
- Liu, L. F. DNA topoisomerase poisons as antitumor drugs. *Annu. Rev. Biochem.* **1989**, *58*, 351–375.
- Chen, A. Y.; Liu, L. F. DNA topoisomerases: essential enzymes and lethal targets. *Annu. Rev. Pharmacol. Toxicol.* **1994**, *34*, 191–218.
- Vladu, B.; Woyrnarowski, J. M.; Manikumar, G.; Wani, M. C.; Wall, M. E.; Von Hoff, D. D.; Wadkins, R. M. 7- and 10-substituted camptothecins: dependence of topoisomerase I–DNA cleavable complex formation and stability on the 7- and 10-substituents. *Mol. Pharmacol.* **2000**, *57*, 243–251.
- Chu, D. T. W.; Hallas, R.; Clement, J. J.; Alder, L.; McDonald, E.; Plattner, J. J. Synthesis and antitumor activities of quinolone antineoplastic agents. *Drugs Exp. Clin. Res.* **1992**, *18*, 275–282.
- Permana, P. A.; Snapka, R. M.; Shen, L. L.; Chu, D. T.; Clement, J. J.; Plattner, J. J. Quinobenzoxazines: a class of novel antitumor quinolones and potent mammalian DNA topoisomerase II catalytic inhibitors. *Biochemistry* **1994**, *33*, 11333–11339.
- Clement, J. J.; Burren, N.; Jarvis, K.; Chu, D. T. W.; Swinarski, J.; Adler, J. Biological characterization of a novel antitumor quinolone. *Cancer Res.* **1995**, *55*, 830–835.
- Fan, J.-Y.; Sun, D.; Yu, H.; Kerwin, S. M.; Hurley, L. H. Self-assembly of a quinobenzoxazine–Mg²⁺ complex on DNA: a new paradigm for the structure of a drug–DNA complex and implications for the structure of the quinolone bacterial gyrase–DNA complex. *J. Med. Chem.* **1995**, *38*, 408–424.
- Yu, H.; Kwok, Y.; Hurley, L. H.; Kerwin, S. M. Efficient, Mg²⁺-dependent photochemical DNA cleavage by the antitumor quinobenzoxazine (S)-A-62176. *Biochemistry* **2000**, *39*, 10236–10246.
- Kwok, Y.; Zeng, Q.; Hurley, L. H. Structural insight into a quinolone–topoisomerase II–DNA complex. Further evidence for a 2:2 quinobenzoxazine–Mg²⁺ self-assembly model formed in the presence of topoisomerase II. *J. Biol. Chem.* **1999**, *274*, 17226–17235.
- Cirilli, M.; Bachechi, F.; Ughetto, G.; Colonna, F. P.; Capobianco, M. L. Interactions between morpholinyl anthracyclines and DNA. The crystal structure of a morpholino doxorubicin bound to d(CGATACG). *J. Mol. Biol.* **1992**, *230*, 878–889.
- Bigi, F.; Casiraghi, G.; Casnati, G.; Sartori, G. Modification of the Nickl reaction. A general synthetic approach to 20-vinyl-2,3-dihydrobenzofurans. *Tetrahedron* **1983**, *39*, 169–174.
- Habib, A. M.; Ho, D. K.; Masuda, S.; McCloud, T.; Reddy, K. S.; Aboushoer, M.; McKenzie, A.; Byrn, S. R.; Chang, C.-J.; Cassady, M. Structure and stereochemistry of psorospermin and related cytotoxic dihydrofuranoxanthones from *Psorospermum febrifugum*. *J. Org. Chem.* **1987**, *52*, 412–418.
- Zeng, Q.; Kwok, Y.; Kerwin, S. M.; Mangold, G.; Hurley, L. H. Design of new topoisomerase II inhibitors based upon a quinobenzoxazine self-assembly model. *J. Med. Chem.* **1998**, *41*, 4273–4278.
- Slapak, C. A.; Kufe, D. W. In *Harrison's Principles of Internal Medicine*, 14th ed.; Isselbacher, K. J., et al., Eds.; McGraw-Hill: New York, 1998; pp 523–537.
- Hurley, L. H. DNA and its associated processes as targets for cancer therapy. *Nat. Rev. Cancer* **2002**, *2*, 188–200.
- Kim, M.-Y.; Duan, W.; Guzman, M.; Hurley, L. H. Design, synthesis, and biological evaluation of a series of fluoroquinolone-thioxazines with contrasting dual mechanisms of action against topoisomerase II and G-quadruplexes. *J. Med. Chem.* **2003**, *46*, 571–583.
- Discover, version 2.9.5 (molecular mechanics force fields), *Insight II* (molecular modeling software); Accelrys Inc., 9685 Scranton Road, San Diego, CA, 92121; 2000.
- Maple, J. P.; Hwang, M.-J.; Jalkanen, K. J.; Stockfish, T. P.; Hagler, A. T. Derivation of class II force fields: V. Quantum force field for amides, peptides, and related compounds. *J. Comput. Chem.* **1998**, *19*, 430–458.
- Cornell, W. D.; Cieplak, P.; Bayly, C. I.; Gould, I. R.; Merz, K. M., Jr.; Ferguson, D. M.; Spellmeyer, D. C.; Fox, T.; Caldwell, J. W.; Kollman, P. A. A second generation force field for the simulation of proteins, nucleic acids, and organic molecules. *J. Am. Chem. Soc.* **1995**, *117*, 5179–5197.
- Luty, B. A.; Wasserman, Z. R.; Stouten, P. F. W.; Hodge, C. N.; Zacharias, M.; McCammon, J. A. A molecular mechanics/grid method for evaluation of ligand–receptor interactions. *J. Comput. Chem.* **1995**, *16*, 454–464.
- Stouten, P. F. W.; Frömmel, C.; Nakamura, H.; Sander, C. An effective solvation term based on atomic occupancies for use in protein simulations. *Mol. Simul.* **1993**, *10*, 97–120.
- Insight II* (molecular modeling software); Accelrys Inc., 9685 Scranton Road, San Diego, CA, 92121; 2000.
- Garemyr, R.; Elofsson, A. Study of the electrostatics treatment in molecular dynamics simulations. *Proteins: Struct., Funct., Genet.* **1999**, *37*, 417–428.
- Orozco, M.; Laughton, C. A.; Herzyk, P.; Neidle, S. Molecular-mechanics modelling of drug–DNA structures: the effects of differing dielectric treatment on helix parameters and comparison with a fully solvated structural model. *J. Biomol. Struct. Dyn.* **1990**, *8*, 359–373.
- Gasteiger, J.; Marsili, M. Iterative partial equalization of orbital electronegativity—a rapid access to atomic charges. *Tetrahedron* **1980**, *36*, 3219–3228.
- Jorgensen, W. L.; Chandrasekhar, J.; Madura, J. D. Comparison of simple potential functions for simulated liquid water. *J. Chem. Phys.* **1983**, *79*, 926–935.

- (41) Andersen, H. C. RATTLE: a "velocity" version of the SHAKE algorithm for molecular dynamics calculations. *J. Comput. Phys.* **1983**, *52*, 24–34.
- (42) Åqvist, J.; Medina, C.; Samuelsson, J. E. A new method for predicting binding affinity in computer-aided drug design. *Protein Eng.* **1994**, *7*, 385–391.
- (43) Åqvist, J. Calculation of absolute binding free energies for charged ligands and effects of long-range electrostatic interactions. *J. Comput. Chem.* **1996**, *17*, 1587–1597.

JM030096I